M.TECH DISSERTATION REPORT

ON

Performance Analysis of Long Hydrodynamic Journal Bearing with Nano Lubricant

BY

NISHANT KUMAR

(2015PDE5127)

UNDER THE SUPERVISION OF

DR. AMIT KUMAR SINGH

DEPARTMENT OF MECHANICAL ENGINEERING,

MALAVIYA NATIONAL INSTITUE OF TECHNOLOGY,

JAIPUR-302017 (RAJASTHAN).

2016-2017

A

DISSERTATION REPORT

ON

Performance Analysis of Long Hydrodynamic Journal Bearing with Nano Lubricant

Submitted in partial fulfillment
of
the requirements for the award of degree of

MASTER OF TECHNOLOGY
IN
DESIGN ENGINEERING

Submitted by

Nishant Kumar
(2015PDE5127)

Supervised by

Dr. Amit Kumar Singh
(Assistant Professor)

DEPARTMENT OF MECHANICAL ENGINEERING,
MALAVIYA NATIONAL INSTITUTE OF TECHNOLOGY,
JAIPUR-302017 (RAJASTHAN)

2016-2017

DEPARTMENT OF MECHANICAL ENGINEERING,
MALAVIYA NATIONAL INSTITUTE OF TECHNOLOGY,
JAIPUR-302017 (RAJASTHAN).

CERTIFICATE

This is to certify that the dissertation work entitled "Performance Analysis of Long Hydrodynamic Journal Bearing with Nano Lubricant" by Mr. Nishant Kumar is a bonafide work completed under my supervision and guidance, and hence approved for submission to the Department of Mechanical Engineering, Malaviya National Institute of Technology in partial fulfillment of the requirements for the award of the degree of Master of Technology with specialization in Design Engineering. The matter embodied in this Seminar Report has not been submitted for the award of any other degree, or diploma.

Place: Jaipur **Dr. Amit Kumar Singh**

Date: 4 July, 2017 **(Assistant professor)**

DEPARTMENT OF MECHANICAL ENGINEERING,
MALAVIYA NATIONAL INSTITUTE OF TECHNOLOGY,
JAIPUR-302017 (RAJASTHAN).

Candidate's Declaration

I hereby certify that the work which is being presented in the dissertation entitled "Performance Analysis of Long Hydrodynamic Journal Bearing with Nano Lubricant", in partial fulfilment of the requirements for the award of the Degree of Master of Technology in Design Engineering, submitted in the Department of Mechanical Engineering, MNIT, Jaipur is an authentic record of my own work carried out for a period of one year under the supervision of Dr. Amit Kumar Singh, Assistant professor of Mechanical Engineering Department, MNIT, Jaipur.

I have not submitted the matter embodied in this dissertation for the award of any other degree.

Place: Jaipur **Nishant Kumar**

Date: 4 July, 2017 **M. Tech (DE)**

ID: 2015PDE5127

Acknowledgement

I express sincere thanks to my supervisor Dr. Amit Kumar Singh, Assistant Professor, Department of Mechanical Engineering, M.N.I.T.,Jaipur., for providing me his invaluable guidance, support, supervision and useful suggestions. I am sincerely thankful to Dr. Dinesh Kumar, Dr. T.C. Gupta and Dr. Himanshu Choudhary who helped me beyond their duty at time of need.

I would also like to thank Mr. Ajit kumar, Mr. Prashant kumar and Mr. Vimal Pathak (Ph.D Research Scholars) for their continuous support and suggestions.

Home is where one starts from; I express my deepest gratitude to my parents and my younger brothers for sharing their love. The motivation I could not find within was rendered to me by them.

Place: Jaipur **Nishant Kumar**

Date: 4 July, 2017 **M. Tech (DE)**

ID: 2015PDE5127

Abstract

The aim of this project is numerical and computational fluid dynamics(CFD) analysis of Hydrodynamic journal bearing with Nanoparticle added lubricating oil. The dynamic analysis of hydrodynamic solid journal bearing operating under nanolubricant will be presented in this paper. The load carrying capacity of solid journal bearing mainly depends upon the thermophysical properties of the Lubricating oil being used. The addition of nanoparticles on commercial lubricants may enhance the viscosity, density, specific heat and thermal conductivity of lubricating oil and in turn changes the performance characteristics. In the proposed work is about to obtain pressure distribution in the clearance space of the solid journal bearing numerically and through ANSYS CFD Fluid Flow(Fluent).

Al_2O_3 nanoparticles are used in this study, $Al_2O_3 + SAE\ 30$ based nano lubricant at various volume fractions, was prepared. The prepared samples exhibit good dispersion stability. The nanolubricant samples with different $Al_2O_3 + SAE\ 30$ volume fractions are then subjected some mathematical calculation to obtain thermophysical properties and hence study the Pressure generation and distribution in lubricating film of hydrodynamic bearing with increasing $Al_2O_3 + SAE\ 30$ nanoparticle concentrations and load acting on bearing. Pressure generation and distribution calculations will be carried out using mathematical modelling of Reynolds equation and CFD fluent flow technique. Calculations will be done at different volume fraction of nanoparticle. Pressure distribution and comparison will be carried out without and with nanoparticle added lubricating oil. The ANSYS software is used to calculate hydrodynamic pressure carrying capacity using dynamic mesh technique.

Contents

List of Figures

Nomenclature

HJB	Hydrodynamic Journal Bearing
θ	Bearing Angle
x	Longitudinal Direction
h	Local oil film thickness
n	Eccentricity ratio
E	Energy
z	Circumferential direction
p	Local oil film pressure
U	Linear velocity
μ	dynamic viscosity
Al	Aluminum
Al_2O_3	Alumina
e	Eccentricity
r	Journal radius
c	Radial clearance
ω	Angular velocity
K	Constant for integration
$h_{p_{min}}$	Thickness of film at minimum pressure
$h_{p_{max}}$	Thickness of film at maximum pressure
p_θ	Pressure at any angle θ

W Load carrying capacity

L Length of the bearing

μ_{nf} Viscosity of nano lubricant

μ_{bf} Viscosity of basic lubricant

φ Volume fraction of nano particle

ρ, ρ_p, ρ_{bf} Density of nano lubricant, nanoparticle and basic lubricant respectively

$c_{p_{nf}}, c_{p_p}, c_{p_{bf}}$ Specific heat of nano lubricant, nanoparticle and basic lubricant respectively

k_{nf}, k_p, k_{bf} Thermal conductivity of nano lubricant, nanoparticle and basic lubricant respectively

g Acceleration due to gravity

$\otimes$ Outer product of any two vector

Chapter-1

Introduction

1.1 Hydrodynamic Journal Bearing

Hydrodynamic bearings are an important element of a rotating machine and are under the sliding system of the simplest structure bearings. Hydrodynamic journal bearings are sliding contact bearings operating in hydrodynamic lubrication. A circular axis called a journal is made to rotate within a fixed sleeve or bush called a bearing.

The liquid bearings were invented by France civil engineer L D Girard, who proposed a railway propulsion system incorporating water-supply hydraulic bearings in 1852. In the late 1880s, an experiment was made on the lubrication of bearing surfaces. Beauchamp Tower's floating experiment and the idea of Osborne Reynolds's theoretical research[1].

Now, the analysis and design of the hydrodynamic journal bearings are attracting a lot of attention to engineers. It is emphasized to design these bearings to avoid metal and metal contact. To design these elements, most important characteristics are predicted, such as load withstanding capacity, maximum pressure, and lubricant flow requirements between the combined surfaces. These parameters can determine when the pressure in the clearance space between the contact faces is known.

The Reynolds equations governing the flow of lubricant in clearance space are used to examine the pressure in the clearance space between the journal and the bearing. The Reynolds equation is only a simplified description of some of the principles of conservation. It is obtained by solving a continuous equation at the same time as a simplistic Navier-Stokes equation. In addition, the accuracy of the results obtained by CFD technology. The main advantage of CFD code is that the full Navier-Stokes equation is used to provide a solution to the flow problem, and the finite difference code is based on the Reynolds equation [2].

In the journal bearing, the lubricant is pulled on the surface of the film itself and moves it into a wedge-shaped zone, creating pressure at a high speed enough to generate the pressure needed to separate the surface against the bearing load. Solid journal bearings are used for heavy machinery and support high loads. A simple journal bearing consists of two Rigid cylinder. The outer tube

(bearing) wraps the inner rotation Journal (axis). The lubricant fills a small annular gap between the journal and the bearing. The eccentricity of the journal is related to the pressure that occurs in bearings to balance the radial load. Lubricant is supplied through a hole or groove, or may not extend over the entire circumference of the journal. The pressure around the journal is measured by various pressure gauges using a pressure tube. This is done at various speeds to get a relationship between speed and pressure [3].

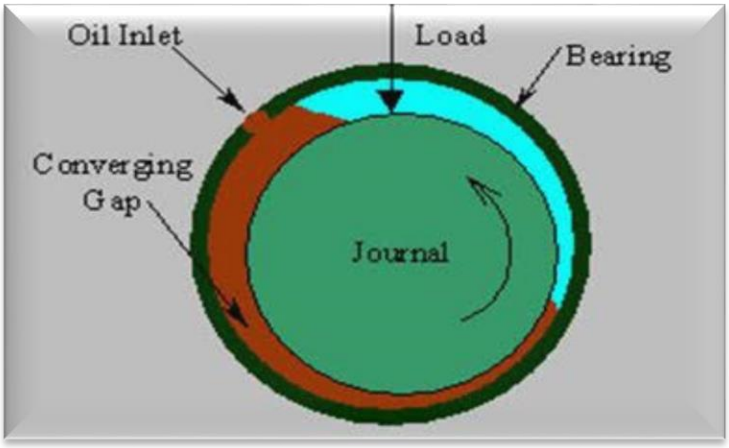

Fig. 1. Schematic of Hydrodynamic Journal Bearing with oil inlet.

In the stationary state of Fig. 2 (a), the radial load W is squeezed lubricant from the clearance space, the metal contact established at point A. When the journal begins rotate and climb the bearing wall by rubbing up to point B. The minimum fluid film thickness, still remains zero in point B as shown in figure 2 (b). When the journal is fast, a wedge-shaped film is formed in B, and as shown in Figure 2 (c), more oil is stretched toward the convergence wedge, and the pressure begins to rise as the journal speed increases. At a specific speed, the pressure generated is sufficient to support the load W, the journal is cast to the opposite side of the vertical load line as shown in Fig. 1 (c) [4].

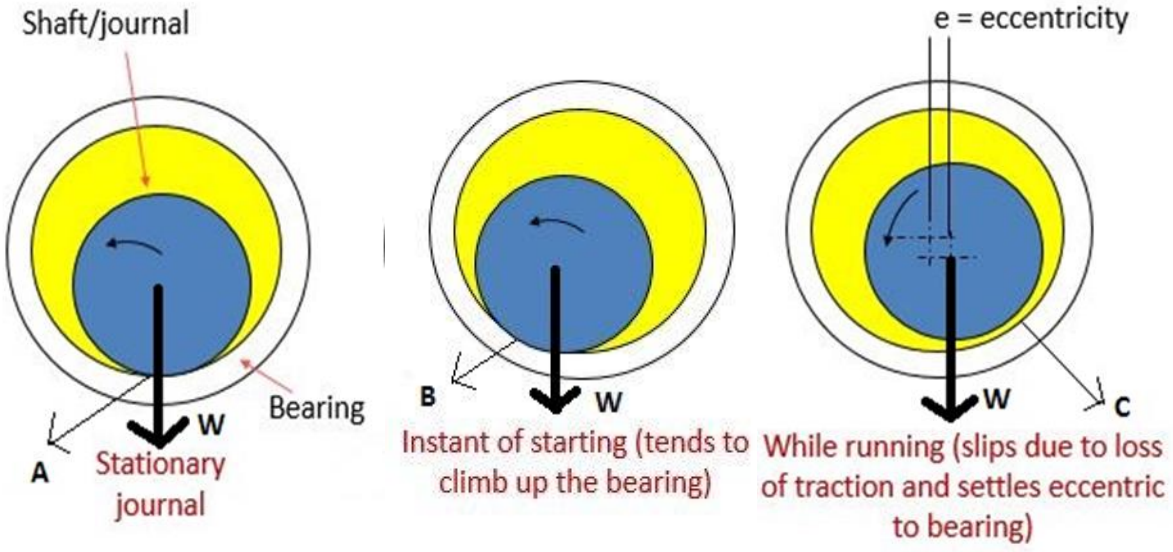

Fig. 2 (a) Fig. 2 (b) Fig.2 (c)

1.1.1 Advantages of Hydrodynamic Journal Bearing

Hydrodynamic Journal Bearing is widely used in different fields because of the following advantages [3]:

- Very low friction (hydrodynamic means that there is a full film of oil between the bearing and race components)
- Lower wear and longer life than standard bearings (no metal-metal contact within the wearing portions of the bearing)
- Should run cooler since there is less friction and mainly viscous loss to the oil
- Perfect lubrication maintained at highest designed shaft speed

1.1.2 Challenges of Hydrodynamic journal bearing

- The correct viscosity of oil is required to avoid contact between metal pieces (temperature and load play into that)
- Hydrodynamic bearings require forced lubrication to maintain the full film
- Costlier than standard bearings
- Starting torque is more

- Pressure of the lubricant need to be increase for given dimension of hydrodynamic journal bearing so that load carrying capacity increases

1.1.3 Applications of Hydrodynamic journal bearing

There are many applications for Hydrodynamic journal bearing in different fields. Some of them are given below.

i. Engineering applications
    a. Turbine shaft
    b. Internal combustion engine crank shaft
    c. Marine engine shaft
    d. Rope conveyors
ii. Aerospace Engineering
    a. Rocket engine turbo pump
    b. Gyro framework bearing
    c. Satellite altitude control bearing
iii. Electrical Engineering
    a. Large size electric motors
    b. Hydroelectric generator
iv. Shipboard applications
    a. Main propeller journals
    b. Turbine generator sets
    c. Clutch
    d. Blowers
    e. Propeller line shafts
    f. Main gear box

1.2 Introduction to Lubricants

Lubricants are substances introduced to reduce friction between surfaces that are in contact with each other, and are usually organic and ultimately reduce the heat generated when the surface

moves. It also has the ability to transmit forces, transport foreign objects, or heat or cool the surface. Characteristics for reducing friction are known as lubricity. The introduction of lubricant to the sliding interface has some beneficial effects on the coefficient of friction. Faced with new developments such as custom synthetic lubricants and additives, many industries continue to work with old spec lubricants. A new understanding of the chemical process provides the possibility of making lubricants for optimal performance in certain applications and improves efficiency and machine safety [5].

Lubricants have been used for thousands of years. Calcium soap has been confirmed in the axle of the tank in 1400 BC. The stone of the building was slid in the wood which impregnated the oil in the age of the pyramid. During the Roman period, lubricants were based on olive oil, rapeseed oils, and animal fats. Using metal-based machines, the Industrial Revolution accelerated the growth of lubrication. Initially, the need for such machinery, which relied on natural oil, was shifted to petroleum-based materials in the early 1900s. The breakthrough was the development of decompression distillation of oil, as described by the vacuum oil company. This technology has made it possible to purify very volatile substances that are common to many lubricants [6].

1.2.1 Hydrodynamic lubrication

Hydrodynamic lubrication is a term that is given when the shaft to be rotated in the bearing is supported by a layer or wedge of oil, if the shaft is not in contact with the bearing material. Hydrodynamic lubrication was first studied by Osborne Reynolds (1842-1912). Reynolds discovered that when the lubricant was applied to the shaft and bearings, the rotating shaft pulled a convergence wedge of lubricant between the shaft and the bearings. He also noted that as the shaft increases in speed, the liquid flows at a faster rate between the two surfaces. This is because the lubricant is viscous, to produce a liquid pressure in the lubricant wedge sufficient to keep the two surfaces separated as shown in Figure 3. Under ideal conditions, Reynolds showed that this liquid pressure was large enough so that the two objects would not be in contact, and that the only friction was the viscous resistance of the lubricant [7].

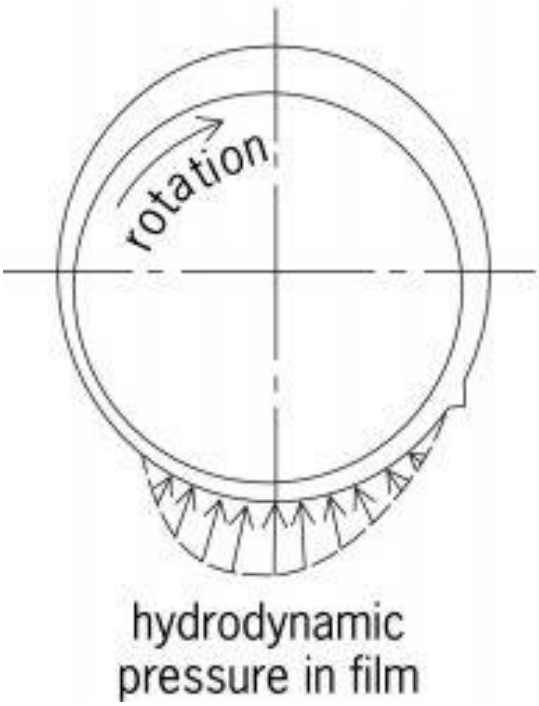

Fig. 3 hydrodynamic operation

1.2.2 Introduction to SAE 30 lubricating oil

Fast journal bearings are always lubricated with oil, not grease. The oil is supplied to the bearing either by a pressurized oil pump system, oil ring or color, or wick. The groove of the bearing shell is used to distribute the oil to the entire surface of the bearing. The choice of lubricant is very important. Because the viscosity of the selected oil is too low, the thickness of the film is insufficient and the heat occurs, and metal and metal contact occurs. If the viscosity of the oil is too high, the heat will occur again, but the internal fluid friction will be generated in the oil.

SAE 30 oil is an oil-based single-grade oil entering the viscosity grade defined by SAE for 30-weight oil. The Automotive Engineers Association (SAE) has established a numerical code system for grading motor oils based on the viscous characteristics of motor oil. Single-grade engine oil is defined as an oil that can't use polymer viscosity index improving agent also referred to as viscosity modifier additive. The SAE 30 is manufactured using a standard golden brown two-color compound and is available in red to easily identify from other oils as needed. When the temperature rises, the kinematic viscosity is lowered. As shown in Figure 4[8], the change in kinematic viscosity and density by temperature.

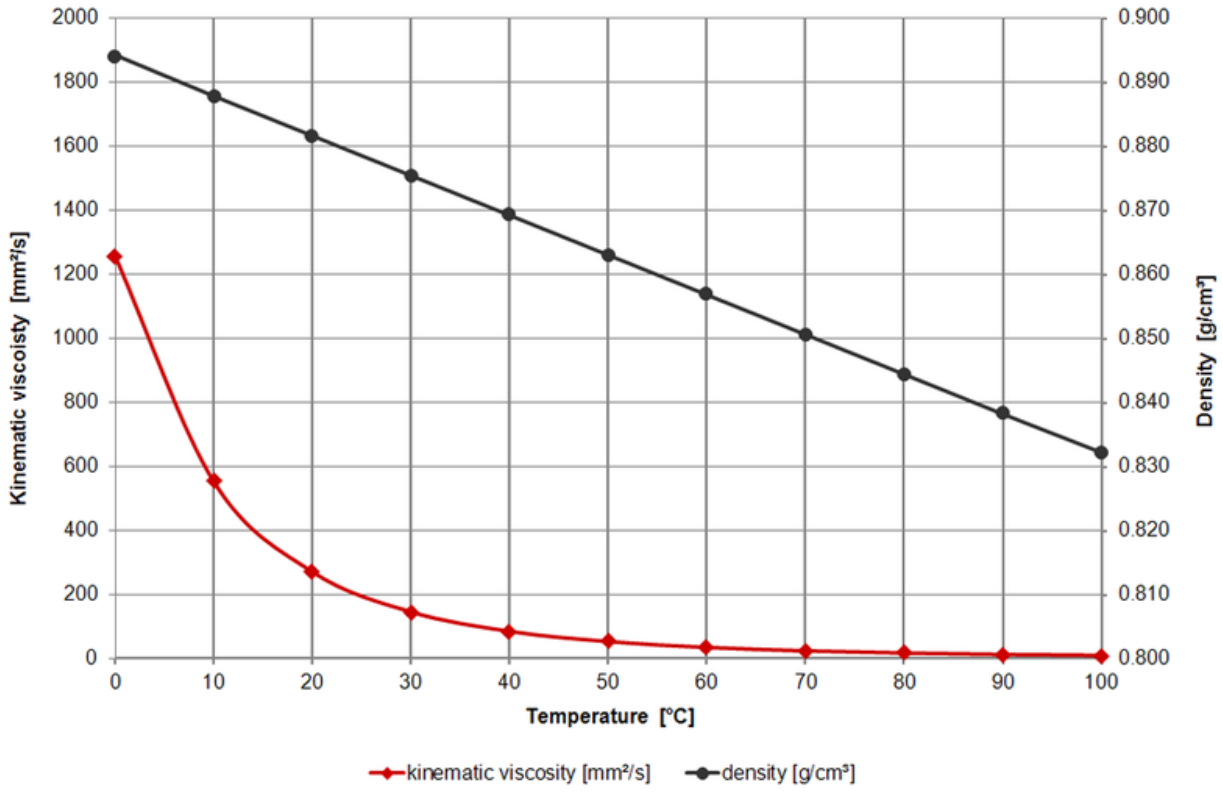

Fig. 4 variation of viscosity and density with temperature

1.3 Introduction to nanolubricant

Nanoparticles are increasingly used in the generation of solutions to modern engineering problems. The processing technology and the preparation method of the nanoparticle are attracting the interest of a huge research. Nanoparticles are small in size, because the specific surface area is very large, has many outstanding properties. Nanoparticles are basically nanometer-sized particles [9].

Nano-lubricant (nanoparticle lubricant suspension) term given by Choi et. al. [10] to describe the heat transfer fluid based on the nanotechnology of these new classes shows the thermal properties superior to the thermal properties of their host fluids. Nano lubricant dispersed in conventional liquids such as ethylene glycol and engine oil, is generally a suspension of metal or metal oxide solid nanoparticles varying in the size of 1 to 100nm. Over the past several decades, there is

increase in interest in nano lubricant i.e. solid nanoparticles of any concentration is liquid dispersed well at a low concentration. Researchers have applied emerging nanotechnology in traditional thermal engineering to develop new career lubricants. Metal or non-metallic nanoparticles has excellent properties including long-term stability and homogeneity, in order to prepare a new type of Nanolubricants, is dispersed in the conventional heat transfer fluid such as water, glycol and oil [11].

The target of the Nanolubricants, by uniform dispersion and stable suspension of the nanoparticles in the host fluid (preferably less than 10nm), as small concentration as possible, preferably to achieve the highest thermal properties possible in less than 1% capacity.

1.3.1 Preparation of nanolubricant

There are two methods used for the preparation of nanolubricants experimentally[9,31]

1. One-step method
2. Two-step method

One-step method, making the particles at the same time in the lubricant, it consists of dispersing. In this method, the drying of nanoparticles, storage, transport, the dispersion of the process is avoided, aggregation of nanoparticles is suppressed to a minimum, the stability of the lubricant is improved. Stage process, it is possible to prepare uniformly dispersed nanoparticles, the particles can be suspended stably in the base fluid.

The two-step method is the most promising method. Nanoparticles used in this method is produced as the first dry powder by chemical or physical method. Then, nano-sized powder, strong magnetic force stirring, ultrasonic stirring, high shear mixing, homogenization, and with the help of a ball mill is dispersed in the lubricant in the second processing process. Since the nano powder synthesis technology has already been expanded to the industrial production level, the two-step method is the most economical method of producing nano-lubricant on a large scale. For high surface area and surface activity, nanoparticles tend to aggregate.

In the literature, it can be found that thermo physical properties of nano lubricant depends on the particle volume fraction and can be expressed by various mathematical expressions.so upon using those equations we can calculate equations for nano lubricant mathematically.

1.3.2 Why Al_2O_3 nanoparticle used

The material of the nanoparticles is chemically stable, the cost is lower than the corresponding metal, it is also readily available, it is selected as Al_2O_3. Its advantages include mechanical strength enhancement and electrical insulation.$Al_2O_3 - SAE$ 30 nano lubricants are prepared in two-step method. Figure 5 shows a transmission electron microscope (TEM) image of the nanoparticles of the diameter 10nm. The image confirms good dispersion, the particles are spherical, although most of them have a diameter of about 10nm or less, indicating those having a diameter of about 50nm [9].

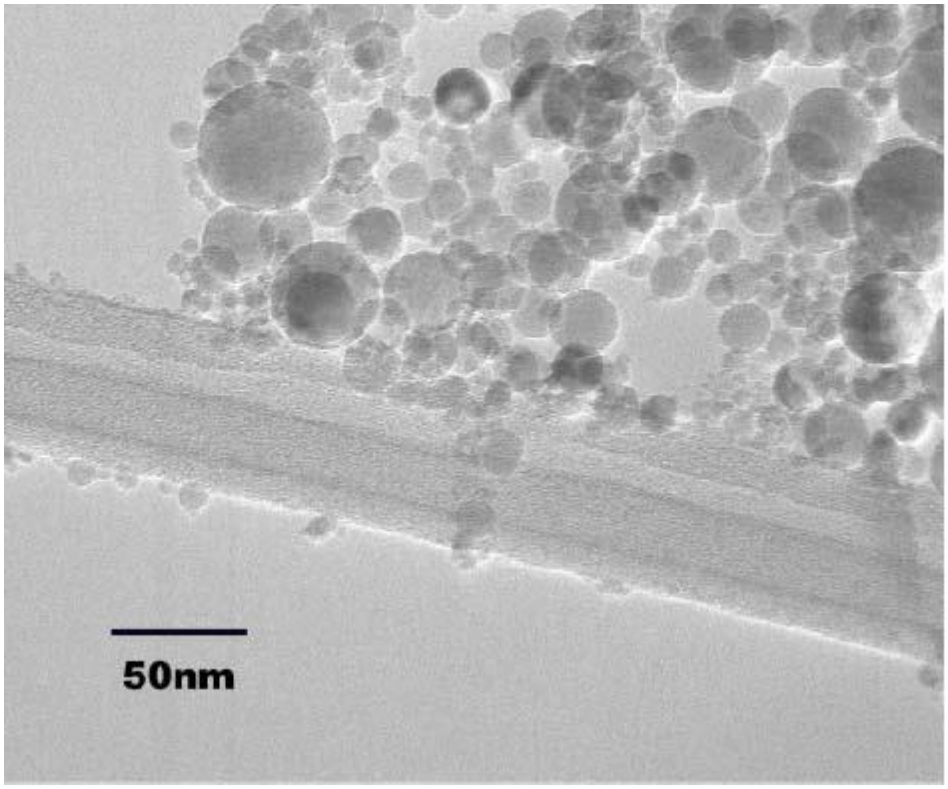

Fig. 5 TEM of Al_2O_3 nanolubricant

1.4 Behavior of hydrodynamic journal bearing with nanolubricants

The load capacity of the hydrodynamic journal Bearings is enhanced by the addition of nanoparticles due to the increase in viscosity of the lubricant, affecting various performance characteristics of the hydrodynamic solid journal bearings. These suspended solid particles increase the thickness of the lubricant, resulting in a variety of performance characteristics of the journal bearing. Addition of nanoparticle in lubricating oil increases the thermos physical properties of lubricant like dynamic viscosity, specific heat, density and thermal conductivity and hence affect the performance of bearing[12,32].

So the use of Nano lubricant in hydrodynamic journal bearing will increase the thermophysical properties and hence improve performance characteristic of bearing as compare to basic lubricant.

Chapter-2

Literature review and objectives

2.1 Literature review

Nano lubricant operated hydrodynamic journal bearing are used extensively in various engineering applications and these are susceptible to poor performance at low and medium speed due to metal to metal contact between journal and bearing, and also it has problem of side leakage. It is also well known that lower is the pressure developed within the lubricant, load carrying capacity of hydrodynamic journal bearing decreases. Therefore, being one of the major design criteria, it is important to study the pressure variation and maximum pressure development within the clearance space between journal and bearing under dynamic condition using various lubricant, such as Nano lubricant for their optimal, accurate and reliable effectiveness. There are numerous studies to date on Nano lubricant behavior on bearing such as $TiO_2 + Water$ nanolubricant $SiC - Demonized\ water$ $Al_2O_3 - Water$ etc. Some tribological relevant works on Nano lubricant study and their behavior on thermo physical property are presented here.

Jiang and Xie [13] investigated the tribological behavior of the conventional metal-containing materials and plasma-sprayed TiO_2 coating pairs with Triphenylthiophosphato and phosphate. As a result, copper-lead alloy paired with TiO_2 coating lubricated with base oil showed optimum tribology performance.

Lee et al. [14] Thermal properties of SiC/DIW nano-fluids for high temperature heat transfer were investigated. Since the characteristics of the nano-lubricant depends on the form of nanoparticles, SiC nano-fluid is prepared in-house, the shape and size of the SiC nanoparticles were also inspected. Because of the *SiC* dispersion stability, the IEP was identified as PH6, and the PH control succeeded in maintaining stability except this point. The maximum relative viscosity measured of 3vol% *SiC*/*DIW* nano-fluid compared with *DIW* was 102%, the maximum relative thermal conductivity data of 3vol% *SiC/DIW* nano-fluid compared with *DIW* was about 7.2%.

Pisal et al. [15] The copper oxide (CuO) nanoparticles studied in his research have been added to the engine oil 20w 40, and Tribology properties have been studied. he was prepared sample of

CuO nanoparticles of various proportions in the engine oil (0.2, 0.5, 0.75 and 1 wt%). The wear and friction experiments were carried out by pin-on-disk Tribometer (pin on disc), and tested by changing the load, speed and concentration of nanoparticles in the engine oil. The results obtained are CuO nanoparticles added to the engine oil shows good friction reduction and abrasion resistance, compared with standard engine oil that does not contain CuO nanoparticles, the friction coefficient at 0.5 wt% concentration was lowered by 24% and 53% respectively. In the friction reduction test, the addition of CuO nanoparticles to the base oil, compared to the oil containing no nanoparticles, the friction coefficient was reduced by 24% and 53% at a concentration of 0.5 wt%.

Y.Y. Wu et al. [16] CuO used as an additive, using TiO_2 and nano-diamond nanoparticles to examine the tribological properties of two lubricants, API-Sf engine oil and base oil. Experimental results show that the nanoparticles added to the Standard Oil, particularly CuO shows good friction reduction and abrasion resistance characteristics. The addition of CuO nanoparticles in Api-Sf engine oil and base oil, the friction coefficient is reduced by 18.4 and 5.8%, respectively, the depth of the wear marks, compared with the Standard Oil without cuo, respectively 16.7 and 78.8% reduced nanoparticles. Furthermore, by using TEM, OM, SEM, we investigated to interpret the possible mechanisms of antifriction and abrasion resistance by nanoparticles.

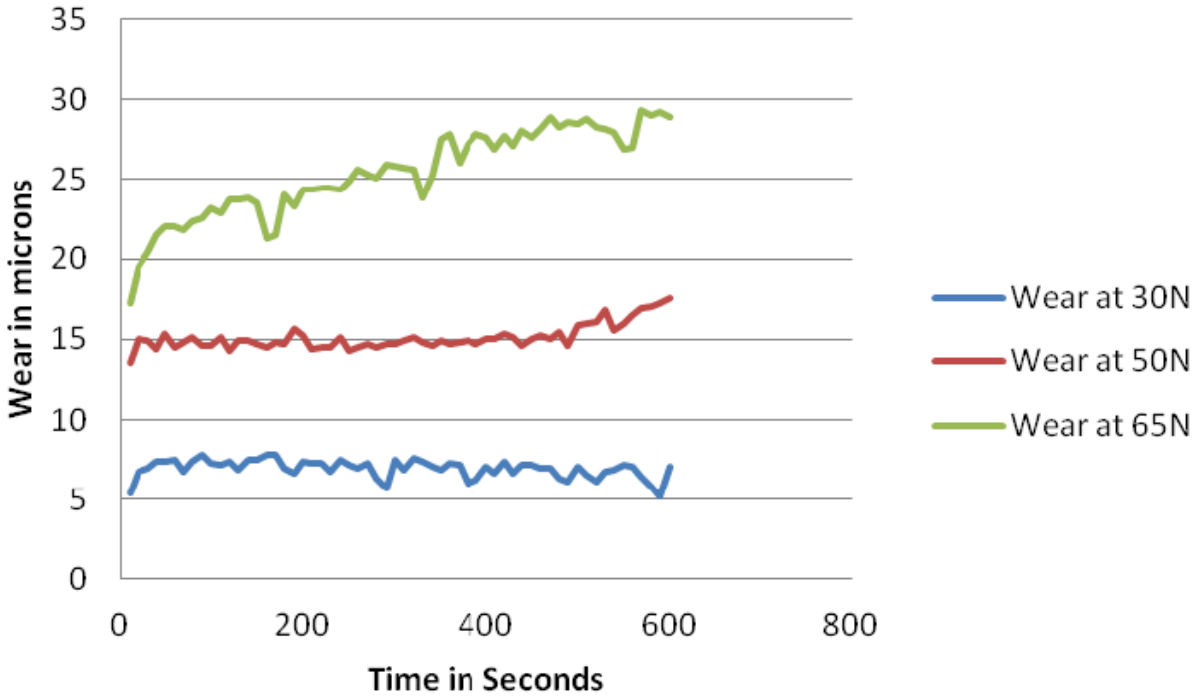

Fig. 6 Wear in micron with base oil without nanoparticles

Binu K.G. et al. [17] the load bearing capacity of the journal bearings, the effect of the shear viscosity fluctuation of the engine oil was studied due to the presence of TiO_2 nanoparticles additive at a volume fraction of 0.005 ~ 0.025. The presence of TiO_2 nanoparticles, even at a low concentration of 0.01 volume fraction, compared to the plain engine oil containing no nanoparticle additive, it was found to increase the load capacity of the journal bearing 40%. DLS granularity analysis reveals that the primary size of the TiO_2 nanoparticles of less than 100nm dispersed in the engine oil form aggregates of the average size 777nm, resulting in the particle filling rate of 7.77. The load carrying capacity of the journal bearing acting on the TiO_2 -based nano-fluid at a constant volume fraction also, it has been found to increase in higher nanoparticle aggregation rate. From the simulation results, when increasing the particle filling rate from 7.77 to 10, it became clear that the load capacity of the TiO_2 nanoparticles concentration of 0.015 volume fraction increases by 35%.

Kalakada et. al.[18] A mathematical model developed for the relationship between the viscosity and temperature of the lubricant Sae15w40 multi-stage engine oil with Al_2O_3 and ZnO nanoparticles was studied. The developed mathematical model for the viscosity and temperature of the lubricant-containing nanoparticles is used to calculate the static performance characteristics of the bearing. These performance characteristics mainly depend on the viscosity of the lubricant. The addition of nanoparticles on the commercially available lubricant, significantly increases the viscosity of the lubricant, then changing the performance characteristics. In order to obtain pressure and temperature distributions, the modified Reynolds and energy equations are used, and these equations are solved using the finite element method. The iteration procedure is used to establish the film range. Performance characteristics are calculated from the pressure field obtained. In the case of non-thermal viscosity, the increase in the weight concentration of the nanoparticles slightly changes the performance characteristics of the bearing. However, in the case of thermal viscosity, the addition of nanoparticles increases the load capacity of the journal bearings of the eccentric rate, this increase is noticeable at a high value of the eccentric rate. **Baskar S. et. al.** [19] In this study, we evaluated the friction and wear behavior of the journal bearing material (brass), and focused on the effect of nano-cuo on chemically modified rapeseed oil. CMRO + 0.5 wt % CuO lubricated bearing material (brass) has the lowest friction coefficient. CMRO + 0.5 W% CuO friction coefficient is 49% smaller than CMRO and 18% lower than Sae20w40. Wear of bearing materials lubricated with Sae20w40, CMRO and Cmro + 0.5 W%

nano-CuO were 86.77, 136.34 and 82.07 mg. The wear value of the bearing material lubricated with CMRO + 0.5 wt% nano-CuO is the lowest abrasion and 39% lower than CMRO. Wear value of bearings lubricated with CMRO + 0.5 W% CuO is 5% lower than Sae20w40. It also has excellent frictional behavior in chemically modified rapeseed oil having a nano-CuO than the other two lubricants. When evaluating the above discussion, among the three lubricants, it is said that it comprises a nano-containing CuO, preferred for lubricating purposes of journal bearing applications.

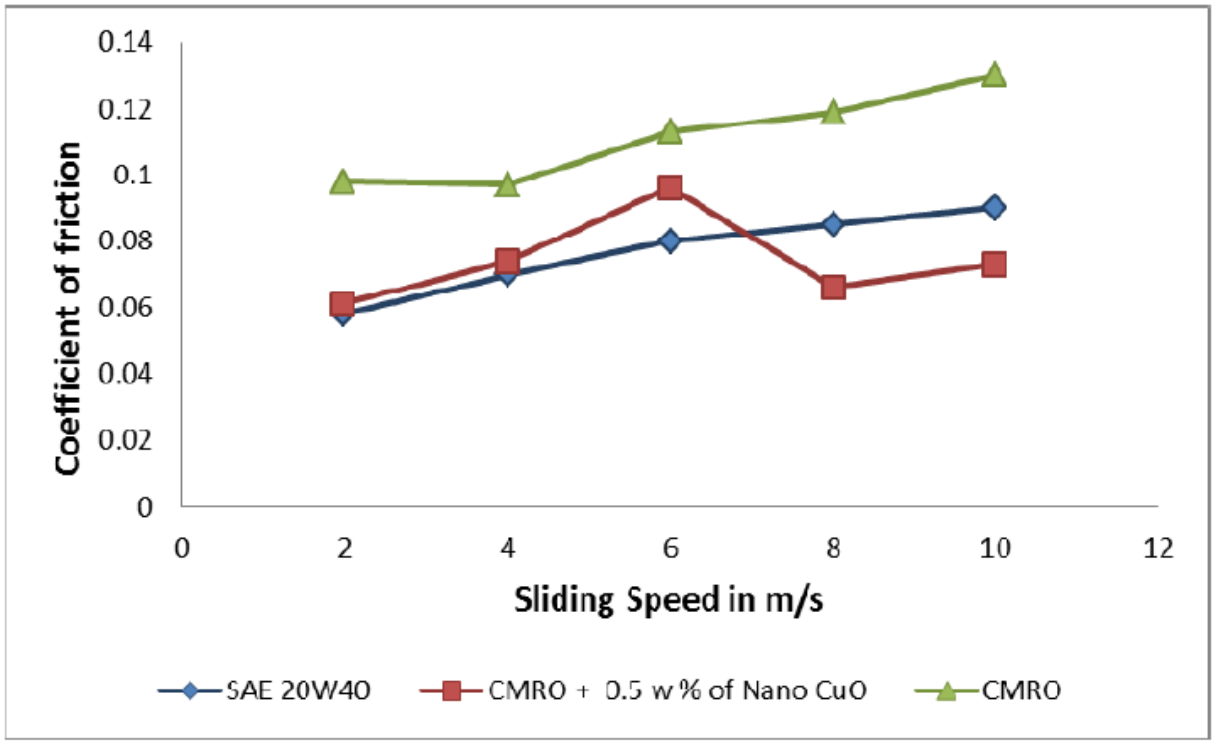

Fig. 7 Coefficient of friction Vs Sliding speed

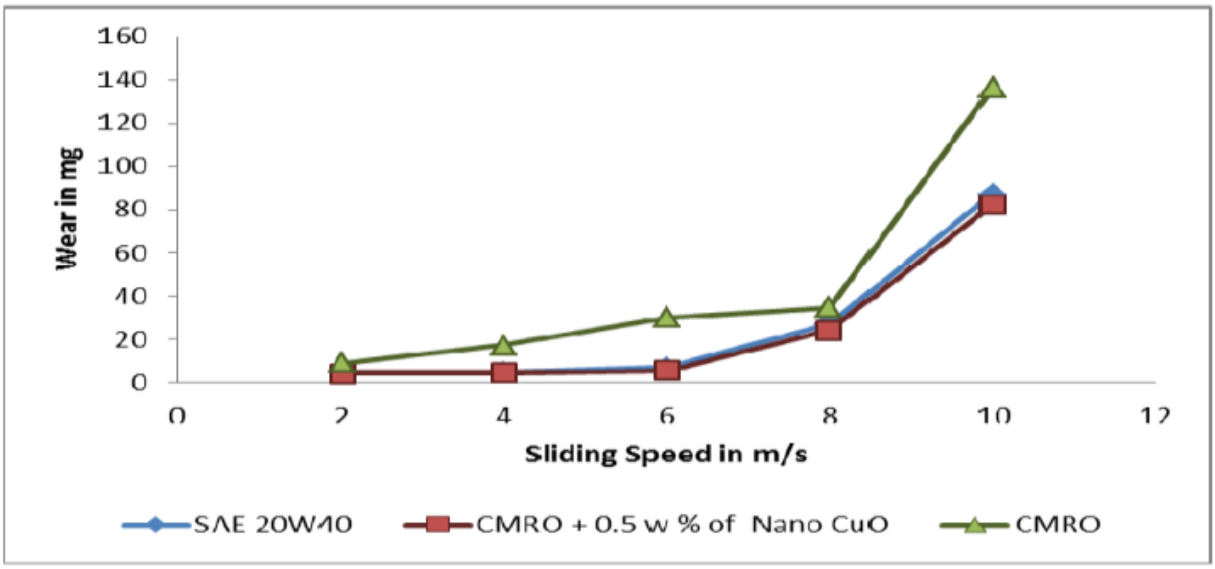

Fig. 8 Wear Vs Sliding speed

The variation of friction coefficient with the duration of rubbing at normal load for SAE20W40, CMRO and CMRO with nano CuO is shown in Fig. 7. The friction coefficient values of brass lubricated with CMRO have higher value than brass lubricated with SAE20W40 and CMRO with nano CuO. The nano CuO dispersed in CMRO has lesser friction coefficient value. From Fig. 7, it can be observed the coefficient of friction decreases by enhancing the nano CuO in CMRO and it shows the lowest value of frictional coefficient of 0.5 % by wt. of nano CuO with CMRO, about 49 % lower than that of CMRO

This might be accredited to the spherical nano CuO producing the rolling medium between pin and disc, when boundary lubrication occurred. However, it is 18 % lower than the coefficient of friction of bearing tribology pair under the influence of synthetic lubricant (SAE20W40) of same viscosity range of CMRO. The addition of nano CuO in CMRO increases the value of wear resistance. The wear values of brass were evaluated and the results are shown in Fig. 8. The brass was lubricated with CMRO had a higher wear value than the other two lubricating oils. The nano CuO in CMRO decreases the value of frictional force.

Yathish K et. al. [20] In his consideration the viscosity change of the lubricant by the addition of TiO_2 nanoparticles as a lubricant additive, it is said that the load capacity of the oil lubricated Biaxial Groove journal bearing is simulated. The shear viscosity of the TiO_2 nanoparticle dispersion in the oil, it is measured for various nanoparticle additive concentration. The results

show an increase in the load capacity of the bearings operating on the nanoparticle dispersion as compared with the plain oil. The presence of TiO_2 nanoparticles of 0.01 volume fraction in engine oil was found to increase the load capacity of 38%. However, the increase in the load capacity should be experimentally verified. The effect of additional particle size on bearing performance also needs to be investigated.

B.S. Shenoy et. al. [21] The static performance characteristics of externally adjustable fluid membrane bearings operating with CuO, TiO_2 and nano-diamond nanoparticle additives in API-Sf engine oil are theoretically simulated. This study has a negative radial direction and negative tilt adjustment bearings with the addition of TiO_2 nanoparticles in particular API-Sf engine oil, the base oil is predicted to bring about 23% and 35% higher load capacity than the API-Sf engine oil containing no nanoparticle additive. In addition, the frictional force of the externally adjustable fluid membrane bearings, as compared with TiO_2 nanoparticle additive, 25% increase for API-Sf engine oil containing no nanoparticles. To examine the change in the load capacity of the fluid film support having a variety of nanoparticle additives, variation of load withstanding capacity with eccentricity ratio for different engine oil is shown in Figure 9.

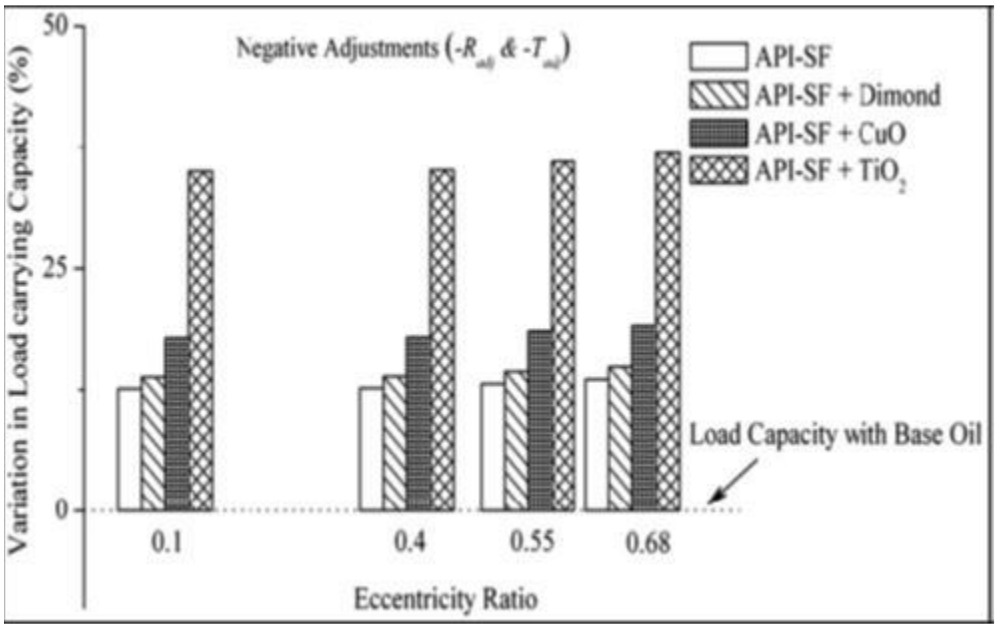

Fig. 9 Variation in Load Carrying Capacity with the addition of nanoparticles additives

Gabi N. et. al. [22] The friction and abrasion performance of ZDDP plain oil additives (0.1% phosphorus) using FEF 3 + Titanium fluoride (3) Catalyst and Polytetrafluoroethylene PTFE were studied using thermal and friction analysis. Thermal weight analysis (TGA), using an X-ray photoelectron spectroscopy (XPS) and ball-on-cylinder wear device, was carried out heat test and tribology test. The effect of TIF3 + FEF3 on the formation and characteristics of abrasion resistant films was investigated. The results showed that the surface of the metal is significantly modified using a fluorine-resistant abrasion additive at a temperature of 100° C, the decomposition temperature of the ZDDP is lowered. This surface modification, a noticeable change in the characteristics, especially the abrasion-protection enhancement and the reduction of surface tension, provide a fluorocarbon and metal fluoride material.

From the literature, it is clear that many studies have been conducted on nanolubricant and their behavior on hydrodynamic journal bearing experimentally and by the use of finite element approach but till date there is no reported CFD technique to analyze the effect of nanolubricant on performance of HJB.so, it was identified as a research gap and this study is CFD based analysis of effect of nanolubricant on the performance of HJB.

2.2 Objectives

- To study the Hydrodynamic pressure variation in a long journal bearing at different bearing angle with conventional lubricant and Nano lubricant numerically.
- Find out the pressure profile between Nano lubricant and conventional lubricant numerical approach.
- To study the Hydrodynamic pressure variation in a long journal bearing with conventional lubricant and Nano lubricant using CFD technique.
- Comparison of maximum pressure in long journal bearing with conventional lubricant and Nano lubricant CFD approach.

Chapter-3

Approach and problem formulation

3.1 Modeling of Hydrodynamic Journal bearing

Existing literature shows that most authors are concerned with the study of static and dynamic performance by changing the geometric shape or lubricant properties of bearings. In this study, we calculate the performance characteristics like pressure distribution, thickness, dynamic coefficient, conveying capacity and attitude angle of hydrodynamic journal bearings. Fig. 10 shows hydrodynamic journal bearing consist of journal and bearing with coordinate system xyz located at the bearing center C, OC is the line of center and obviously, the minimum and maximum oil film thickness are along the line called attitude line. In the present study, hydrodynamic analysis of journal bearing with Nano lubricant is shown[3].

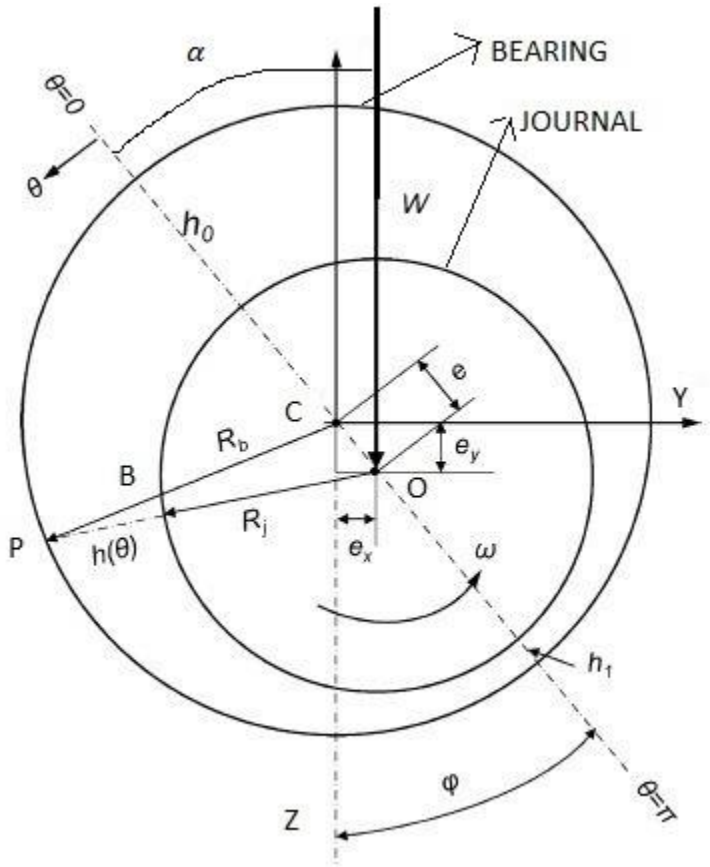

Fig. 10. Hydrodynamic long journal bearing

3.2 Mathematical formulation of Hydrodynamic Journal Bearing

Present analysis explores enhancing the pressure carrying capacity of hydrodynamic journal bearing using Reynold's equation and CFD techniques. The principle of hydrodynamic lubrication was first established by the well-known scientist Osborne Reynolds, and he described the mechanism of hydrodynamic lubrication by generating a viscous liquid film between the moving surfaces. Journal bearing design parameters such as pressure capacity can be determined from the Reynolds equation numerically.

.3.2.1 Reynolds Equation

The lubricant pressure distribution as a function of journal speed, bearing geometry, oil clearance and lubricant viscosity is described by the Reynolds equation. The viscosity is assumed to be constant throughout the oil film, the lubricant is a Newtonian, it is incompressible, the flow is assumed to be laminar flow. The governing equation is[23]

$$\frac{\partial}{\partial x}\left[h^3\frac{\partial p}{\partial x}\right]+\frac{\partial}{\partial z}\left[h^3\frac{\partial p}{\partial z}\right]=6\mu U\frac{\partial h}{\partial x}+12\mu\frac{\partial h}{\partial t} \quad (1)$$

3.2.2 Infinite Long Bearing

In case of infinite long bearing, the flow of lubricant in axial direction or in longitudinal direction of the bearing can be neglected and for steady state operating condition, the Reynolds equation is modified as [4,24]

$$\frac{\partial}{\partial z}\left[h^3\frac{\partial p}{\partial z}\right]=6\mu U\frac{\partial h}{\partial x} \quad (2)$$

From the fig. 10 we can consider the bearing to be fixed and the journal rotates at constant angular velocity $\omega\, rad/sec$ .PB is the film thickness across any radius inclined at any angle θ from the attitude line. O is the center of journal.

$$\boldsymbol{OC = e,} \quad \boldsymbol{h = (r + c) - CB,}$$

Where:

$$\boldsymbol{CB = \sqrt{r^2 - e^2 sin^2\theta} - ecos\theta} \tag{3}$$

From equation (2),

$$\boldsymbol{h = r + c - \sqrt{r^2 - e^2 sin^2\theta} - ecos\theta} \tag{4}$$

The term $\boldsymbol{e}$ is less (less than 1) so $\boldsymbol{e^2}$ is very less so it can be neglected, the term $\boldsymbol{e^2 sin^2\theta}$ under the square root is neglected, hence finally

$$\boldsymbol{h = c + ecos\theta}$$

$$\boldsymbol{h = c(1 + ncos\theta)} \tag{5}$$

Where:

$$\boldsymbol{n = \frac{e}{c}}$$

Assuming

$$\boldsymbol{z = r\theta} \quad \text{so,} \quad \boldsymbol{\partial z = r\partial\theta} \tag{6}$$

$$\boldsymbol{U = r\omega}$$

Upon substituting the value of equation (6) in equation (2), we have

$$\frac{\partial}{\partial\theta}\left[h^3\frac{\partial p}{\partial\theta}\right]=6\mu\omega r^2\frac{\partial h}{\partial\theta} \tag{7}$$

3.2.3 Mathematical Model of Long Journal Bearing

Upon integrating the equation (7), we have

$$h^3\frac{\partial p}{\partial\theta}=6\mu\omega r^2\int\frac{\partial h}{\partial\theta}d\theta \tag{8}$$

$$h^3\frac{\partial p}{\partial\theta}=6\mu\omega r^2 h+K \tag{9}$$

Upon substituting value of h form equation (5) to equation (9), we have

$$\frac{\partial p}{\partial\theta}=\frac{6\mu\omega r^2}{c^2}\left[\frac{1}{(1+n\cos\theta)^2}+\frac{K}{c(1+n\cos\theta)^3}\right] \tag{10}$$

Integrating again equation (10), we have

$$p=\frac{6\mu\omega r^2}{c^2}\left[\int\frac{d\theta}{(1+n\cos\theta)^2}+\int\frac{Kd\theta}{c(1+n\cos\theta)^3}\right] \tag{11}$$

From the fig. 10, we conclude that

$p_{\theta=2\pi}=p_{\theta=0}$

$i.e.,$

$$p_{\theta=2\pi}-p_{\theta=0}=0 \tag{12}$$

Now equation (11) modified as

$$\int_0^{2\pi} \frac{d\theta}{(1+n\cos\theta)^2} + \frac{K}{c}\int_0^{2\pi} \frac{d\theta}{(1+n\cos\theta)^3} = 0 \qquad (13)$$

Therefore,

$$\frac{K}{c} = \left[-\int_0^{2\pi} \frac{d\theta}{(1+n\cos\theta)^2} \right] / \left[\int_0^{2\pi} \frac{d\theta}{(1+n\cos\theta)^3} \right] \qquad (14)$$

Assuming

$$I_1 = \int_0^{2\pi} \frac{d\theta}{(A+\cos\theta)}$$

Which is

$$I_1 = 2\int_0^{\pi} \frac{d\theta}{(A+\cos\theta)} \qquad (15)$$

Differentiating $equation\ (15)\ with\ respect\ to\ \boldsymbol{A}$, we have

$$\frac{dI_1}{dA} = \int_0^{2\pi} \frac{d}{dA}\left(\frac{1}{A+\cos\theta}\right) d\theta$$

$$\frac{dI_1}{dA} = -\int_0^{2\pi} \frac{d\theta}{(A+\cos\theta)^2} \qquad (16)$$

Where

$$A = \frac{1}{n}$$

Similarly, Let

$$\boldsymbol{I_2 = \int_0^{2\pi} \frac{d\theta}{(1+ncos\theta)^2}}$$

$$\boldsymbol{I_2 = A^2 \int_0^{2\pi} \frac{d\theta}{(A+cos\theta)^2}}$$

Then

$$\boldsymbol{I_2 = \frac{dI_1}{dA} A^2}$$

Similarly, Let

$$\boldsymbol{I_3 = \int_0^{2\pi} \frac{d\theta}{(1+ncos\theta)^3}}$$

$$\boldsymbol{I_3 = A^3 \int_0^{2\pi} \frac{d\theta}{(A+cos\theta)^3}}$$

Then

$$\boldsymbol{I_3 = -\frac{1}{2}\frac{dI_2}{dA} A^3}$$

Let

$$\boldsymbol{t = tan\frac{\theta}{2} \qquad so, \qquad \frac{2dt}{(1+t^2)} = d\theta} \tag{17}$$

Upon substituting the value of equation (17) in equation (15), we have

$$\boldsymbol{I_1 = \left[\frac{A}{\sqrt{A^2-1}} \tan^{-1}\left(\sqrt{\frac{A-1}{A+1}}\, tan\frac{\theta}{2}\right)\right] \quad from\ 0\ to\ \frac{\pi}{2}}$$

Upon solving

$$\boldsymbol{I_1 = \frac{2\pi}{\sqrt{A^2 - 1}}} \tag{18}$$

This gives

$$\boldsymbol{I_2 = \frac{2\pi A^3}{(A^2 - 1)\sqrt{A^2 - 1}}}$$

$$\boldsymbol{I_3 = \frac{\pi(2A^3 + 1)A^3}{(A^2 - 1)^2\sqrt{A^2 - 1}}}$$

Therefore

From $\boldsymbol{I_1, I_2\ and\ I_3}$

The value of

$$\boldsymbol{K = 2c(n^2 - 1)/(2 + n^2)} \tag{19}$$

3.2.4 Location of Maximum Pressure

From equation (10), we find that

$$\boldsymbol{\frac{dp}{d\theta} = 0} \quad \textit{when} \quad \boldsymbol{K = -c(1 + ncos\theta)}$$

and from equation (5)

$$\boldsymbol{K = -h}$$

So, the location of maximum and minimum pressure is given by

Film thickness(h) as

$$\boldsymbol{h_m = h_{p=min,max} = -K = 2c(1 - n^2)/(2 + n^2)} \tag{20}$$

As,

$$-K = h$$

$$c(1 + ncos\theta) = 2c(1 - n^2)/(2 + n^2)$$

$$cos\theta = \frac{-3n}{(n^2 + 2)} \tag{21}$$

3.2.5 Pressure Distribution

Equation (11) can be written as

$$p_\theta = p_0 + \frac{6\mu\omega r^2}{c^2}\left[\int_0^\theta \frac{d\theta}{(1 + ncos\theta)^2} - \int_0^\theta \frac{h_m d\theta}{c(1 + ncos\theta)^3}\right] \tag{22}$$

Let

$$A = \frac{1}{n}$$

Then equation (22) modified as

$$p_\theta = p_0 + \frac{6\mu\omega r^2 A^2}{c^2}\left[\int_0^\theta \frac{d\theta}{(A + cos\theta)^2} - \frac{h_m A}{c}\int_0^\theta \frac{d\theta}{(A + cos\theta)^3}\right] \tag{23}$$

Further assuming

$$J_1(\theta) = \int_0^\theta \frac{d\theta}{(A + cos\theta)}$$

$$J_2(\theta) = \int_0^\theta \frac{d\theta}{(A + cos\theta)^2}$$

$$J_3(\theta) = \int_0^\theta \frac{d\theta}{(A + cos\theta)^3}$$

Then,

$$J_2(\theta) = \frac{-d}{dA}[J_1(\theta)] = \frac{-d}{dA}\left[\frac{A}{\sqrt{A^2-1}}\tan^{-1}\left(\sqrt{\frac{A-1}{A+1}}\ tan\frac{\theta}{2}\right)\right]$$

$$J_2(\theta) = \frac{2A}{(A^2-1)\sqrt{A^2-1}}\tan^{-1}\left(\sqrt{\frac{A-1}{A+1}}tan\frac{\theta}{2}\right) - \frac{1}{A^2-1}\frac{sin\theta}{A+cos\theta} \quad (24)$$

And

$$J_3(\theta) = -\frac{1}{2}\frac{d}{dA}[J_2(\theta)]$$

$$= \frac{2A^2+1}{(A^2-1)^2\sqrt{A^2-1}}\tan^{-1}\left(\sqrt{\frac{A-1}{A+1}}tan\frac{\theta}{2}\right) - \frac{3A}{2(A^2-1)^2}\frac{sin\theta}{A+cos\theta}$$

$$- \frac{sin\theta}{2(A^2-1)(A+cos\theta)^2} \quad (25)$$

Upon using equation (23) and value of $J_1(\theta)$, $J_2(\theta)\ and\ J_3(\theta)$, we have[4]

$$p_\theta - p_0 = \frac{6\mu\omega r^2}{c^2}\left[\frac{n(2+ncos\theta)sin\theta}{(2+n^2)(1+ncos\theta)^2}\right] \quad (26)$$

Equation (26) gives pressure distribution in the infinite long hydrodynamic journal bearing

3.2.6 Load Carrying Capacity

The load carrying capacity of infinite long journal bearing is determined from equilibrium condition perpendicular to the attitude line,

i. e.,

$$W = Lr \int_0^{2\pi} p_\theta \, sin\theta \, d\theta$$

$i.e.,$

$$W = \frac{6\mu\omega r^3 Ln}{c^2(2+n^2)} \int_0^{2\pi} \frac{(2+ncos\theta)sin^2\theta}{(1+ncos\theta)^2} d\theta \qquad (27)$$

Let

$$t = 1 + ncos\theta$$

$$sin\theta = \frac{1}{n}\sqrt{(n^2-1)+2t-t^2}$$

$$d\theta = -\frac{dt}{n\sqrt{(n^2-1)+2t-t^2}}$$

Upon integrating equation (27) with the help of above expressions, we have

$$W = \frac{12\pi\mu\omega r^3 Ln}{c^2(2+n^2)\sqrt{1-n^2}} \qquad (28)$$

Equation (28) gives the load carrying capacity in the infinite long hydrodynamic journal bearing

3.2.7 Half Sommerfeld Condition

The pressure distribution in equation (26) is always positive in the convergent portion of the film giving the necessary wedge action to support the load. However, the pressure in divergent portion of the oil film may be negative which cannot be supported by oil film therefore it is conventional to account for the oil film in the convergent wedge portion alone and neglect the diverging wedge. Such a condition is called Half Sommerfeld Condition.[24]

For Half Sommerfeld condition:

$$p_\theta - p_0 = \frac{6\mu\omega r^2}{c^2}\left[\frac{n(2+n\cos\theta)\sin\theta}{(2+n^2)(1+n\cos\theta)^2}\right] \qquad for\ 0 \le \theta \le \pi$$

$$p_\theta - p_0 = 0 \qquad for\ \pi \le \theta \le 2\pi \qquad (29)$$

3.3 Thermo-physical Properties of Nano lubricant

The characteristics of the nano-lubricant varies depending on the size and volume ratio of the nanoparticles in the base fluid. Nano lubricant can be considered a liquid-solid mixture of nanoparticles suspended in pure fluid. The presence of these particles, the thermal properties of the nano-lubricant is different from pure fluid. The relevant properties are thermal conductivity, viscosity, heat capacity and density. In the literature, these characteristics depend on the volume fraction of the particles and expressed as

3.3.1 Viscosity of Nano lubricant

The Einstein equation, which is suitable for small rigid spherical particles in the volume fraction of less than 0.02, was used to estimate the viscosity of Nano lubricants [25]:

$$\mu_{nf} = \mu_{bf}(1 + 2.5\varphi) \qquad (30)$$

Brinkman has extended Einstein formula to the following form useful to moderate particle suspension

$$\mu_{nf} = \mu_{bf}\left(\frac{1}{(1-\varphi)^{2.5}}\right) \qquad (31)$$

3.3.2 Density of Nano lubricant

Density of Nano lubricant is given by[25]

$$\rho = \varphi\rho_p + (1-\varphi)\rho_{bf} \qquad (32)$$

3.3.3 Specific Heat of Nano lubricant

Specific heat of Nano lubricant is given by[25]

$$C_{p_{nf}} = \frac{\varphi(\rho c_p)_p + (1-\varphi)(\rho c_p)_{bf}}{\rho_{nf}} \tag{33}$$

3.3.4 Thermal Conductivity of Nano lubricant

Thermal Conductivity of Nano lubricant is given by[25]

$$K_{nl} = k_{bf}\left(\frac{k_p + 2k_{bf} + 2\varphi(k_p - k_{bf})}{k_p + 2k_{bf} - \varphi(k_p - k_{bf})}\right) \tag{34}$$

3.4 Computational Fluid Dynamics(CFD) Analysis

Computational fluid dynamics (CFD) can simultaneously predict fluid flow, energy transfer and pressure variation in the bearing. A CFD model is built upon fundamental physical equations of fluid flow and energy transfer. This technology can provide a time-dependent and steady solution to the combined differential equations that control the flow of fluids. Its main benefits are: Combined with the ability to express the effects of very complex shapes and solving complex flow problems, physics is based more on basic modeling. Since then, it has been developed and applied to more and more diverse issues such as automobiles, aerospace, nuclear engineering, turbo machines, biomedical fields, buildings, the environment, and Fire safety engineering [26].

However, there are many assumptions and approximations for both creating and building CFD tools and applying them to specific flow problems. It is also necessary to achieve reasonable execution time and often compromises. They all ultimately affect the trust that can be placed on the results of CFD simulations. With the help of CFD technology, you can calculate the pressure distribution in the journal bearings and modify the design with the corresponding information. CFD technology enables rapid and inexpensive analysis of fluid flow and their behavior for different parameters of hydrodynamic journal Bearings.

3.4.1 ANSYS Fluent Tool

ANSYS Fluent is the most powerful computational fluid dynamics (CFD) software tool and can respond more quickly to optimize product performance. Fluent includes validated physical modeling capabilities to provide fast and accurate results across a wide range of CFD and Multi physics Applications.

ANSYS provides a comprehensive set of computational fluid mechanics software for modeling fluid flow and other related physical phenomena. Provides unparalleled fluid flow analysis capabilities, and provides all the tools you need to design and optimize new fluid equipment and troubleshoot existing equipment. The main ANSYS products in the fluid field are ANSYS fluent. These solutions enable you to simulate a wide range of phenomena, such as aerodynamics, combustion, fluid dynamics, liquid/solid/gaseous mixtures, particle dispersion, reaction flow, and heat transfer. Steady state and transient flow phenomena are easily and quickly resolved [29, 30]

3.4.2 Process involved in CFD

When applying a CFD package to undertake a flow and thermal analysis, there are number of steps that involved for completing the CFD process.

1. Defining the geometry and domain
2. Selecting physical sub-models
3. Specifying boundary conditions at the walls, window openings and material properties.
4. Discretizing the mathematical equations, Create a mesh (divide space into small volumes), set the time step (split time into discrete steps), and include a selection of sub-models of numbers.
5. Monitoring the iterative solution process.
6. Analyzing the solution obtained
7. Uncertainties that may arise at each of these steps are highlighted
8. Visualize the obtained solution.

3.4.3 Governing equations

Governing equations (Navier-stokes equations) are important in any fluid flow problems. Governing equations are two types, compressible and incompressible. To build a mathematical representation of a 3d model and numerically solve the 3-d Navier-stokes equations over a discretized flow field based on the finite volume method. Incompressible N-S equations were used for simulating the "fluid flow movement and their behavior". N-S Equations; conservation of mass, momentum equation, and energy equations are described below[26]

3.4.3.1 Conservation of Mass

In the case of a steady flow situation, the conservation of mass equation states that what flows in must come out. The equation is written as:

$$\frac{\partial}{\partial t}(\rho \boldsymbol{u}) + \nabla.(\rho \boldsymbol{u} \otimes \boldsymbol{u}) = -\nabla.p\boldsymbol{I} + \nabla\boldsymbol{\tau} + \rho \boldsymbol{g} \qquad (35)$$

The first term describes the density changes with time and the second term defines the mass convection, where "u" is the vector describing the velocity in the u, v and w directions.

3.4.3.2 Momentum Equation

The equation of momentum is obtained by applying the Newton's second law that the rate of the momentum of the fluid element equals the sum of the force acting on it. The equation is written as:

$$\rho\left(\frac{\partial \boldsymbol{u}}{\partial t} + (\boldsymbol{u}.\nabla)\boldsymbol{u}\right) = -\nabla \boldsymbol{p} + \nabla.\boldsymbol{\tau} + \rho \boldsymbol{g} + \boldsymbol{f} \qquad (36)$$

Here, the left side represents an increase in momentum and inertia force, and the right side includes the force to act on it. These forces include the pressure p, gravity g, the external force vector f, and the scale of the viscous stress tensor τ acting on the fluid in the control volume. In these forces, gravity is most important because it represents the effect of buoyancy on the flow.

3.4.3.3 Conservation of Energy

The energy conservation equation is the first law of thermodynamics, and the increase of the energy of the control volume is equal to the amount of work done by the expansion is subtracted from heat. Energy equation is

$$\left(\frac{\partial}{\partial t}(\rho E) + \nabla.(v(\rho E + p))\right) = \nabla.\left(k_{eff}\nabla T - \sum_j h_j J_j + (\tau_{eff}.v)\right) + S_h \quad (37)$$

Where:

$$E = h - \frac{p}{\rho} + \frac{v^2}{2}$$

The first three terms on the right side of the upper equation represent the energy transfer by conduction, species diffusion, and viscous dissipation, and S_h contains heat and other defined volume heat sources of the chemical reaction.

Chapter-4

Analysis of Hydrodynamic Journal Bearing using Nano lubricant

Pressure and Load distribution analysis, of long hydrodynamic journal bearing with various volume fraction of Nano lubricant is carried out using half Sommerfeld method based on Reynolds equation and computational fluid dynamic is based on ANSYS fluent flow. The lubricant flowing through the gap between journal and bearing is assume to be Newtonian, incompressible and laminar regime. Based upon half Sommerfeld condition for long journal bearing a plot between pressure carrying capacity and bearing angle is drawn using MATLAB and through computational fluid dynamic(CFD) technique. The accuracy of present formulation is verified by comparing the results obtained from the present model with the available results in literature. Parametric studies are conducted to examine the effects of Nano lubricant on the performance of long hydrodynamic journal bearing.

4.1 Verification of results

The accuracy of the developed program is checked by comparing the results obtained from the present formulation with those available in the literature [27]. The pressure distribution of long hydrodynamic journal bearing (*L/D ratio* = 2.5), with length of bearing (*L=0.125 m),* diameter of journal (*D=0.*05 *m*), radial clearance ($2.5 * 10^{-5}m$) , eccentricity ($1.25 * 10^{-5}m$) , speed (1000 r. p. m) and dynamic viscosity of oil (*0.19 Pa-sec) are compared* with Mane et al. [27], and the corresponding results of validation are shown in Fig.11. It can be seen by Fig.11 that the plot between pressure distribution and bearing angle obtained by present formulation (taking eccentricity $1.25 * 10^{-5}m$), matches well with that reported by Mane et al.(2013).[27].

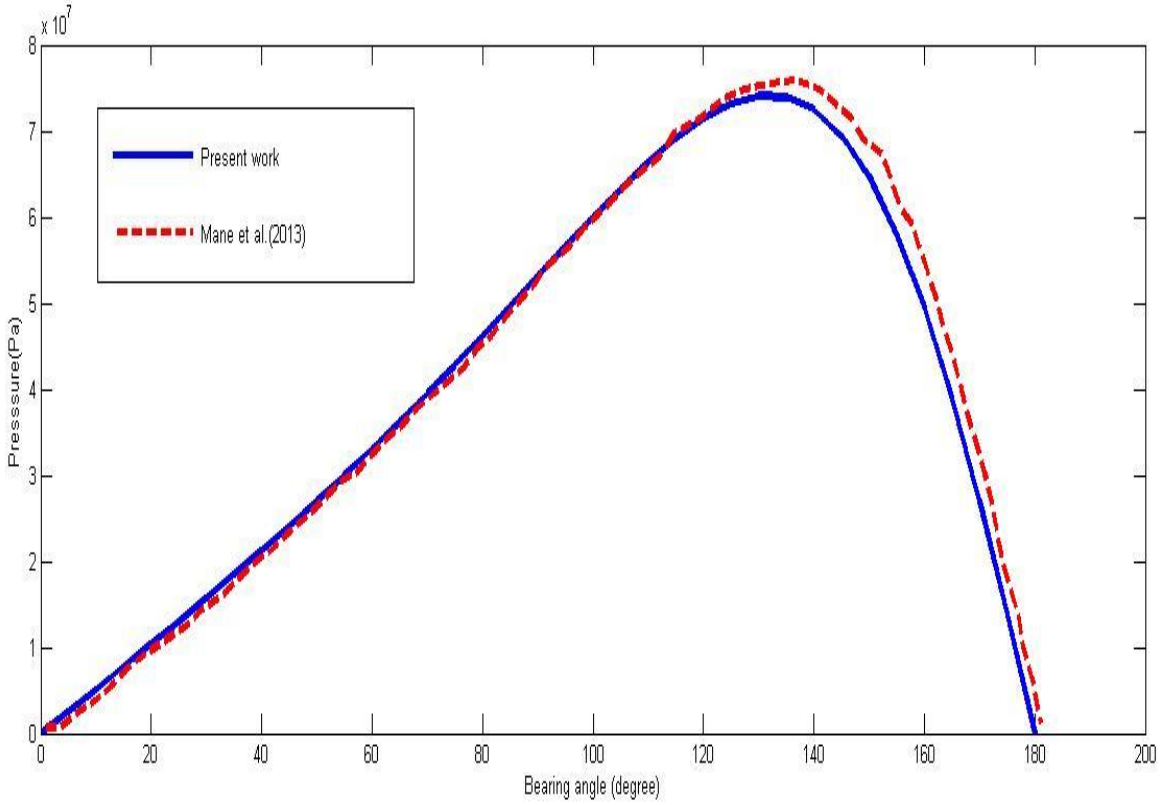

Fig. 11 Comparison of pressure distribution for long journal bearing obtained in the present study with Mane et al.(2013)[27]

4.2 Present numerical studies

In this section, various numerical studies conducted to examine the effects of $Al_2O_3 - SAE\ 30$ nanolubricant on the performance of long hydrodynamic journal bearing. Initially $SAE\ 30$ lubricating oil is taken into the long journal bearing and performance of long journal bearing is analyzed like pressure carrying capacity, load carrying capacity of the bearing. Upon using certain boundary conditions and equation (29) a curve between pressure and bearing angle, load carrying capacity and bearing angle is plotted using MATLAB code. Again $Al_2O_3 - SAE\ 30$ nanolubricant with volume fraction of 0.01 of Al_2O_3 nanoparticle is taken and dynamic viscosity of nanolubricant is calculated using equation (30) given by Einstein and value of this dynamic viscosity is kept in equation (29), a curve between pressure and bearing angle, load carrying capacity and bearing

angle is plotted using MATLAB code. Finally $Al_2O_3 - SAE\ 30$ nanolubricant with volume fraction of 0.04 of Al_2O_3 nanoparticle is taken and dynamic viscosity of nanolubricant is calculated using equation (31) given by Brinkman and value of this dynamic viscosity is kept in equation (29), a curve between pressure and bearing angle, load carrying capacity and bearing angle is plotted using MATLAB code. At last, comparative study is carrying out.

4.2.1 Effect of nanoparticle

The effect of nanoparticle is to increase the viscosity of lubricant as these suspended solid particles increase thickness of lubricants. When volume fraction of nanoparticle is less than 0.02 then the effect of turbulence, Brownian motion is not considered hence below 0.02 volume fraction of nanoparticle Einstein's linear formula is used but when volume fraction of nanoparticle increase beyond 0.02 then Brownian motion of particle become significant and Einstein's linear formula is modified as Brinkman formula as shown in fig. 12. So two separate volume fraction based study is carried out to know the effect of nanoparticle[25].

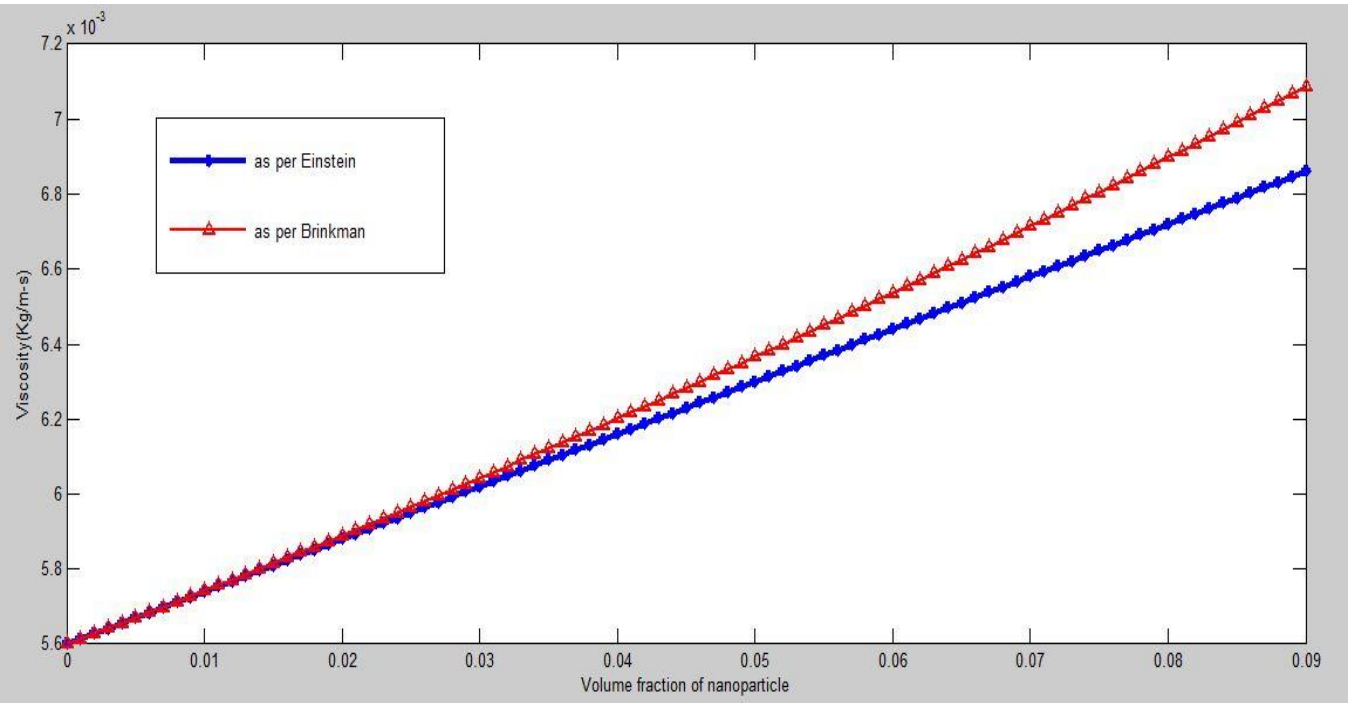

Fig. 12 variation of viscosity with volume fraction of nanoparticle

4.2.2 Thermophysical properties of Al_2O_3 nanoparticle

For Al_2O_3 nanoparticle (*size 25nm*), corresponding thermophysical properties are as[25]

Density$(\rho) = 3970\ kg/m^3$,Thermal conductivity(k)$= 46\ W/mK$

Specific Heat$(c_p) = 750\ J/kgK$

4.2.3 Thermophysical properties of SAE 30 lubricant

For SAE 30 lubricant, corresponding thermophysical properties are as[28]

Density$(\rho) = 872\ kg/m^3$,Thermal conductivity(k)$= 0.135\ W/mK$

Specific Heat$(c_p) = 1800\ J/kgK$, Dynamic viscosity$(\mu) = 0.0056 Kg/m-s$

4.3 Numerical results and discussion

In this section, the steady state analysis of plain journal bearings has been carried out for the case of infinitely long journal bearing with constant length to diameter ratio(L/D=2.5). Length of bearing(L) is taken as 0.125 m, Diameter of journal(D) is 0.05 m, radial clearance(c) between journal and bearing is taken as $2.5 * 10^{-3} m$, eccentricity(e) is taken as 0.0006 m, eccentricity ratio(n=e/c) is 0.24, the speed with which journal is rotated as 3000 r.p.m (314.16 rad/sec).

The viscosity of SAE 30 lubricant is taken from section 4.2.3 and viscosity of $Al_2O_3 - SAE$ 30 nanolubricant with volume fraction 0.01 is calculated with the help of equation (30) and section 4.2.3, so viscosity obtained is $0.00574\ kg/m-s$. Similarly, viscosity of $Al_2O_3 - SAE$ 30 nanolubricant with volume fraction 0.04 is calculated with the help of equation (31) and section 4.2.3, so viscosity obtained is $0.006201\ kg/m-s$.Upon using equation (29) and given above data curves are plotted between pressure distribution and bearing attitude angle, for SAE 30 lubricant, $Al_2O_3 - SAE$ 30 nanolubricant with volume fraction 0.01 and $Al_2O_3 - SAE$ 30 nanolubricant with volume fraction 0.04 using Matlab as shown in fig. 13.it can be seen from fig. 13, the maximum pressure when long journal bearing operated with SAE 30 lubricant at bearing angle 110° is 0.2634 KPa. The maximum pressure when long journal bearing operated with

$Al_2O_3 - SAE\ 30$ nanolubricant with volume fraction 0.01 at bearing angle 110° is 0.2699 KPa and with $Al_2O_3 - SAE\ 30$ nanolubricant with volume fraction 0.04 maximum pressure at bearing angle 110° is 0.2916 KPa.

	$SAE\ 30\ lubricant$	$Al_2O_3 - SAE\ 30\ Nano$ Lubricant with 0.01 volume fraction of Al	$Al_2O_3 - SAE\ 30\ Nano$ Lubricant with 0.04 volume fraction of Al
Bearing angle (θ) in degree	Pressure (KPa)	Pressure(KPa)	Pressure (KPa)
10	0.03128	0.03206	0.03464
20	0.0624	0.06396	0.0691
30	0.09317	0.09549	0.1032
40	0.1233	0.1264	0.1366
50	0.1525	0.1563	0.1689
60	0.1802	0.1847	0.1995
70	0.2057	0.2109	0.2278
80	0.2281	0.2339	0.2526
90	0.2462	0.2524	0.2727
100	0.2586	0.2650	0.2863
110	0.2634	0.2699	0.2916
120	0.2589	0.2653	0.2866
130	0.2434	0.2495	0.2695
140	0.2158	0.2212	0.2389
150	0.1758	0.1802	0.1947
160	0.1246	0.1277	0.1380
170	0.06466	0.06628	0.0716

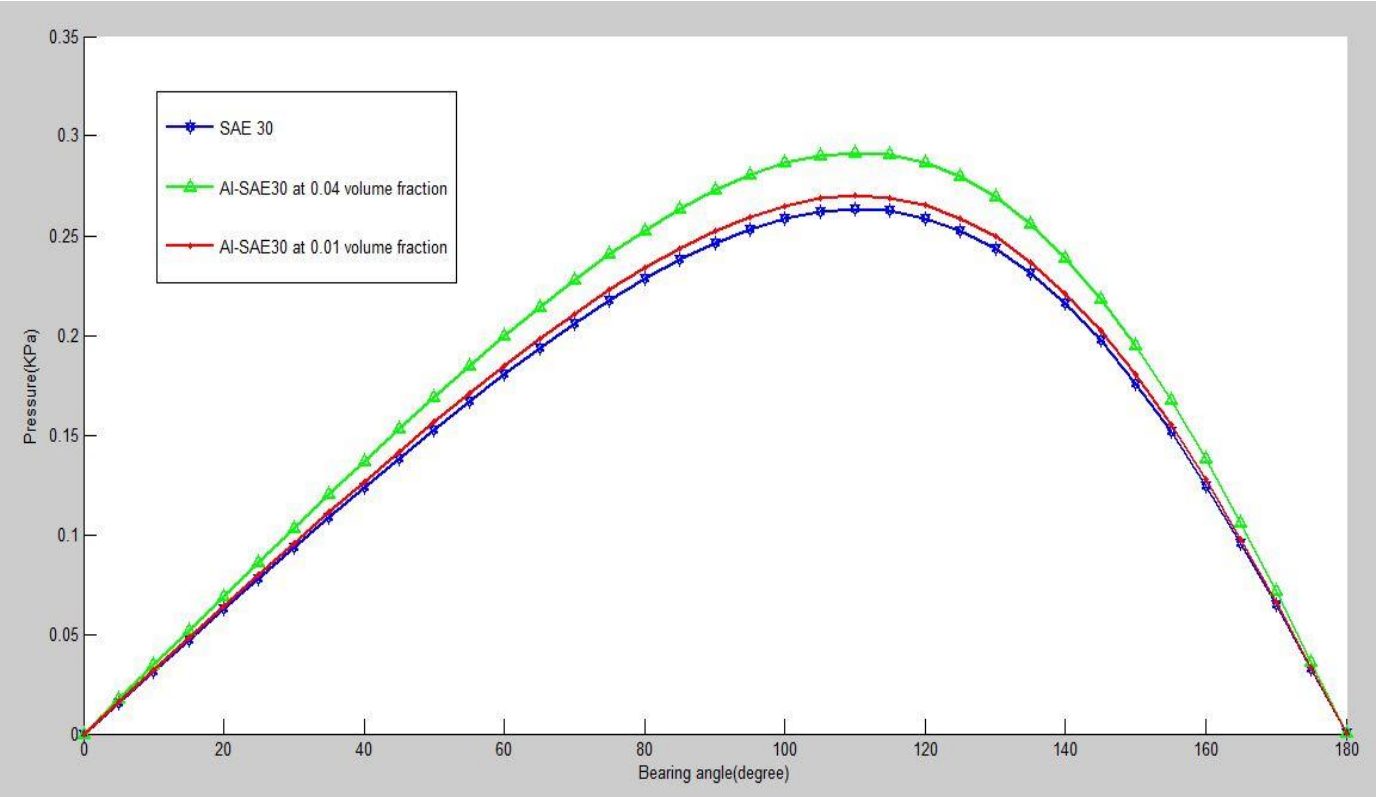

Fig. 13 pressure distribution for LJB using half Sommerfeld condition at eccentricity ratio, n = 0.24

Upon using equation (28) and given above data curves are plotted between load carrying capacity and journal speed for $SAE\ 30$ lubricant, $Al_2O_3 - SAE\ 30$ nanolubricant with volume fraction 0.01 and $Al_2O_3 - SAE\ 30$ nanolubricant with volume fraction 0.04 using Matlab as shown in fig. 14.it can be seen from fig. 14, with increase in speed of journal, load carrying capacity of long journal bearing increases and for the given speed with increase in the volume fraction of nanoparticle load carrying capacity of long journal bearing increases, so for the given dimension of long hydrodynamic journal bearing use of nanolubricant is more effective in order to enhance the load carrying capacity.

	$SAE\ 30\ lubricant$	$Al_2O_3 - SAE\ 30\ Nano$ Lubricant with 0.01 volume fraction of Al	$Al_2O_3 - SAE\ 30\ Nano$ Lubricant with 0.04 volume fraction of Al
Speed of Journal (r.p.m)	Load (N)	Load (N)	Load (N)
500	0.4151	0.4254	0.4596
1000	0.8301	0.8509	0.9192
1500	1.245	1.276	1.379
2000	1.66	1.702	1.838
2500	2.075	2.127	2.298
3000	2.49	2.553	2.758
3500	2.905	2.978	3.217
4000	3.32	3.403	3.677
4500	3.735	3.829	4.136
5000	4.151	4.254	4.596

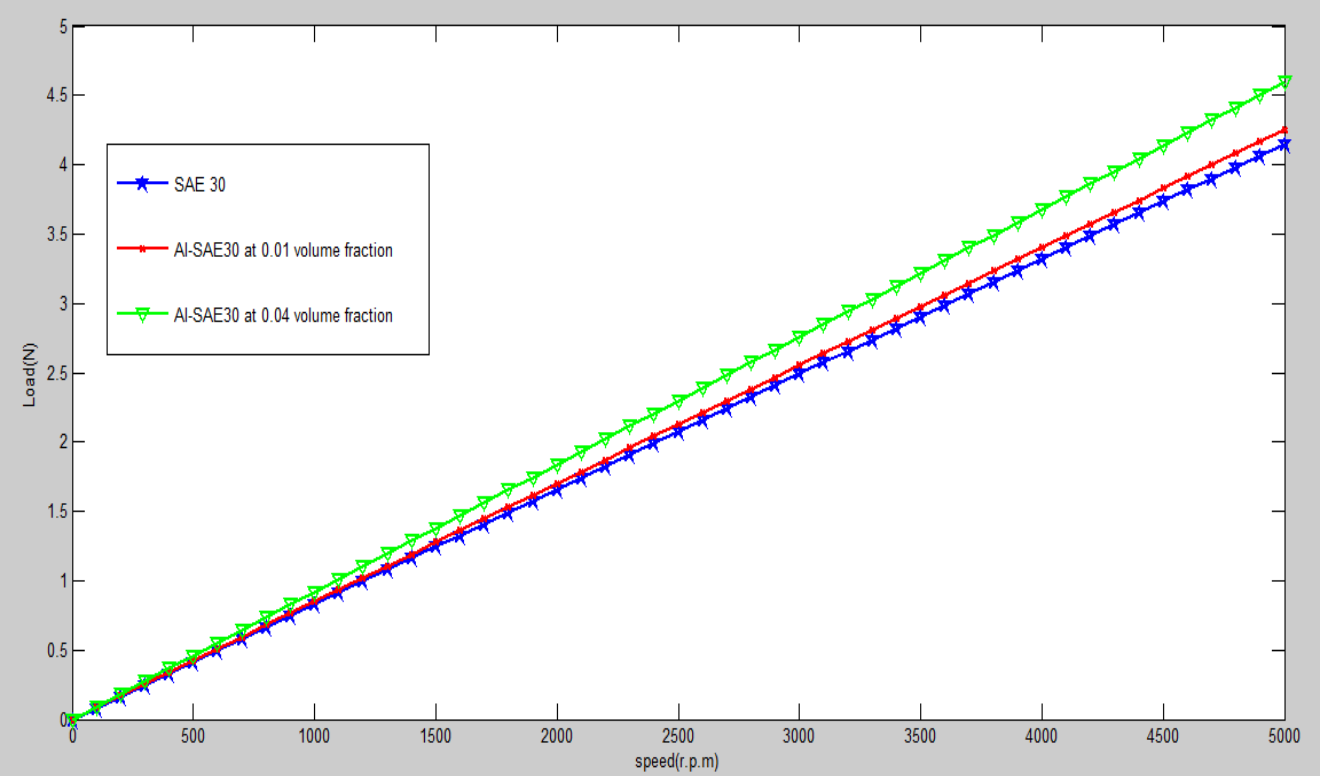

Fig. 14 load distribution for LJB at eccentricity ratio, n = 0.24

4.4 Present Computational Fluid Dynamic(CFD) studies

A 3-D simulation model is developed using the ANSYS CFD package fluid flow(Fluent). various computational fluid dynamic simulation studies conducted to examine the effects of $Al_2O_3 - SAE\ 30$ nanolubricant on the performance of long hydrodynamic journal bearing, pressure based analysis under transient condition and performance characteristic was noted down after 30 minutes of operation of long journal bearing. To proceed in this analysis, first a 3-dimensional bearing has been generated with the help of AUTODESK INVENTOR professional 2016.material for fluid is used as $Al_2O_3 - SAE\ 30$ nanolubricant at different volume concentration of nanoparticle. Initially Al_2O_3 lubricating oil thermophysical properties are taken in material section of CFD fluid flow fluent and maximum pressure developed in lubricant is noted down after 30 minutes of operation, again $Al_2O_3 - SAE\ 30$ nanolubricant with volume concentration of 0.01 thermophysical properties are taken in material section of CFD fluid flow fluent and maximum pressure developed

in lubricant is noted down after 30 minutes of operation, same process is repeated for nanolubricant with 0.04 volume fraction. At last, comparative study is carrying out.

4.4.1 Verification of results

The accuracy of the developed simulation is checked by comparing the results obtained from the present formulation with those available in the literature [27]. The pressure distribution of long hydrodynamic journal bearing (*L/D ratio* = 2.5), with length of bearing (*L=0.125 m)*, diameter of journal (*D=0.*05 *m*), radial clearance ($2.5 * 10^{-5} m$) , speed (1000 r. p. m) i.e 2.617 m/sec and dynamic viscosity of oil is taken as 0.19 Pa-sec *are compared* with Mane et al. [27], and the corresponding results of validation are shown in Fig.15 and Fig.16. It can be seen by Fig.15 and Fig.16 that maximum pressure obtained by present formulation matches well with that reported by Mane et al.(2013).[27].

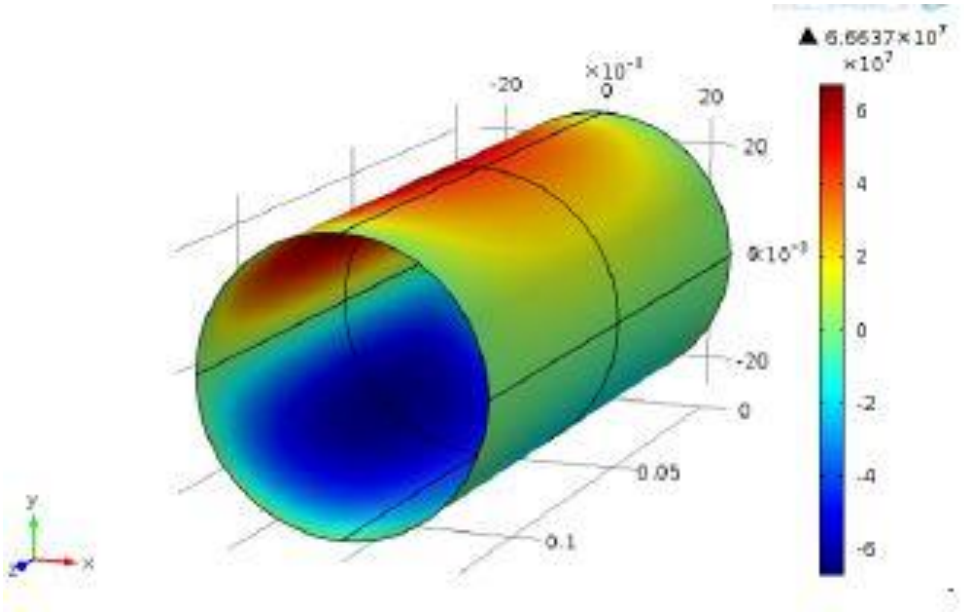

Fig. 15 pressure contour as per Mane et al.(2013)[27]

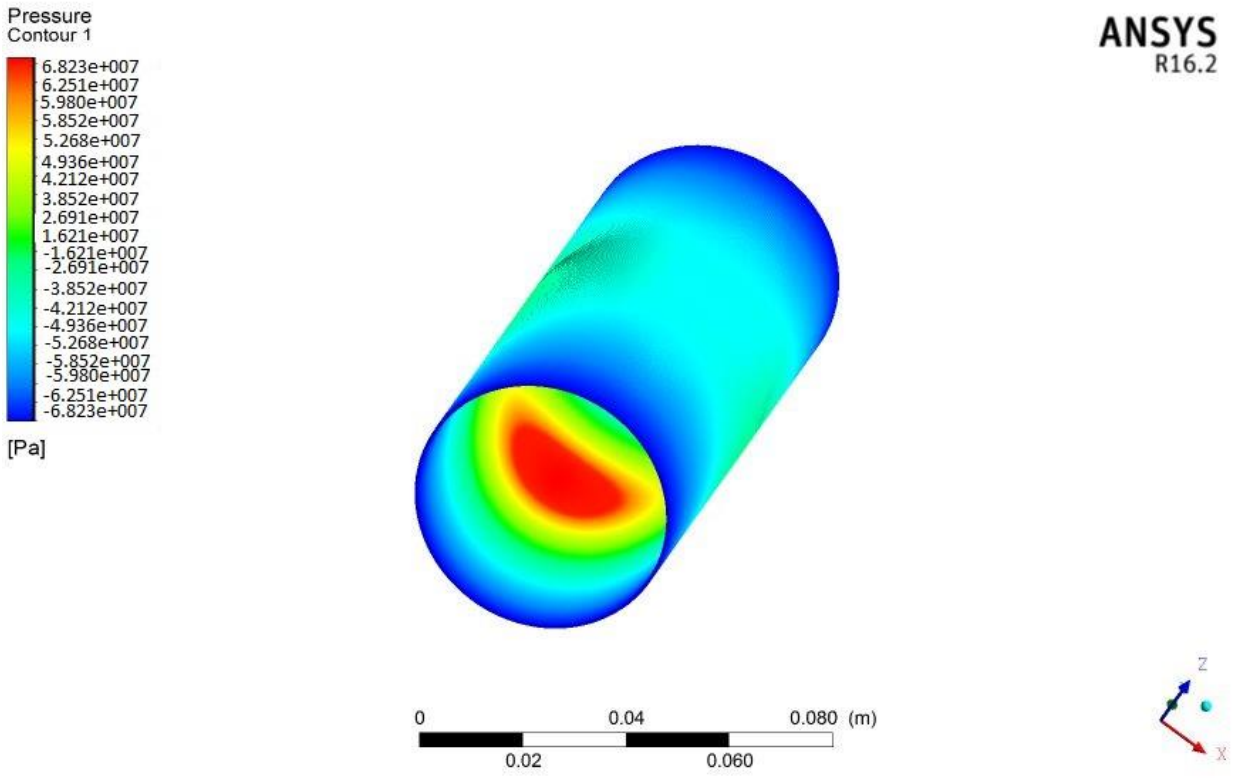

Fig. 16 pressure contour as per present work

4.4.2 Boundary conditions

1. type of inlet is velocity inlet with velocity of 7.85 m/sec
2. At the inlet initial gauge pressure is 101325 Pa
3. gauge pressure at outlet 1(at L=0) is zero
4. gauge pressure at outlet 2(at L=125 mm) is zero

4.4.3 CFD results and discussion

In this section, the transient analysis of plain journal bearings has been carried out for the case of infinitely long journal bearing for 30 minutes operation having the same dimension of journal bearing is taken from section 4.4.1 but the speed of journal is taken as 3000 r.p.m(7.85 m/sec) and the operating temperature is 315 K.

The thermophysical properties like viscosity, density, specific heat and thermal conductivity of $SAE\ 30$ lubricant is taken from section 4.2.3 and thermophysical property of $Al_2O_3 - SAE\ 30$ nanolubricant with volume fraction 0.01 is calculated with the help of equation (30),(32),(33) and

(34) and section 4.2.2 & 4.2.3, so viscosity obtained as 0.00574 $kg/m-s$, density obtained as 902.98 Kg/m^3 , thermal conductivity as 0.139 $W/m-K$,and specific heat obtained as 1753.83 J/KgK .Similarly, thermophysical properties of Al_2O_3-SAE 30 nanolubricant with volume fraction 0.04 is calculated with the help of equation (31),(32),(33) and (34) and section 4.2.2 & 4.2.3, so viscosity obtained as 0.006201 $kg/m-s$, density obtained as 995.92 Kg/m^3 , thermal conductivity as 0.151 $W/m-K$,and specific heat obtained as 1632.57 J/KgK. Upon using the given above data and boundary condition, maximum pressure is calculated for SAE 30 lubricant, Al_2O_3-SAE 30 nanolubricant with volume fraction 0.01 and Al_2O_3-SAE 30 nanolubricant with volume fraction 0.04 using ANSYS R 16.2 Fluid flow(Fluent) as shown in fig. 17, fig.18 and fig. 19. it can be seen from fig. 17,fig. 18 and fig. 19, the maximum pressure when long journal bearing operated with SAE 30 lubricant is 4.495 $*$ 10^6 Pa . The maximum pressure when long journal bearing operated with Al_2O_3-SAE 30 nanolubricant with volume fraction 0.01 is 5.050 $*$ 10^6 Pa and maximum pressure with Al_2O_3-SAE 30 nanolubricant with volume fraction 0.04 is 5.461 $*$ 10^6 Pa.

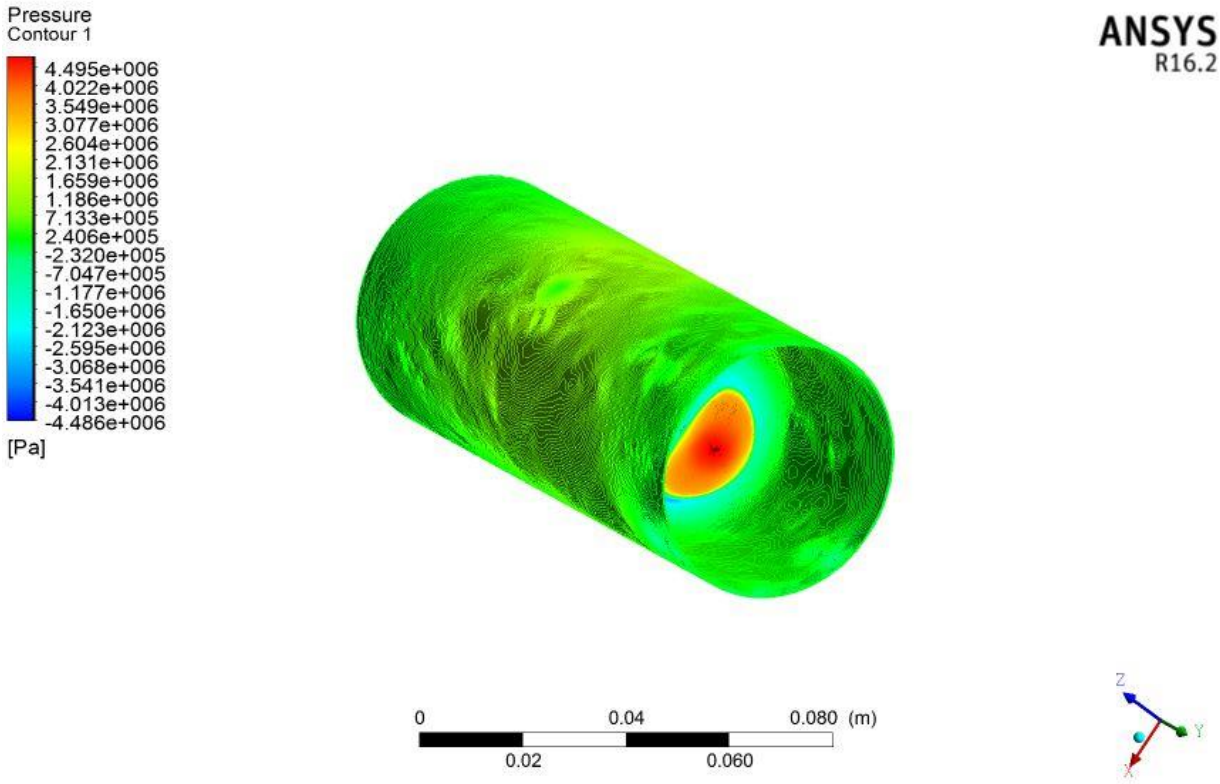

Fig. 17 Pressure contour on Journal surface with SAE 30 lubricant

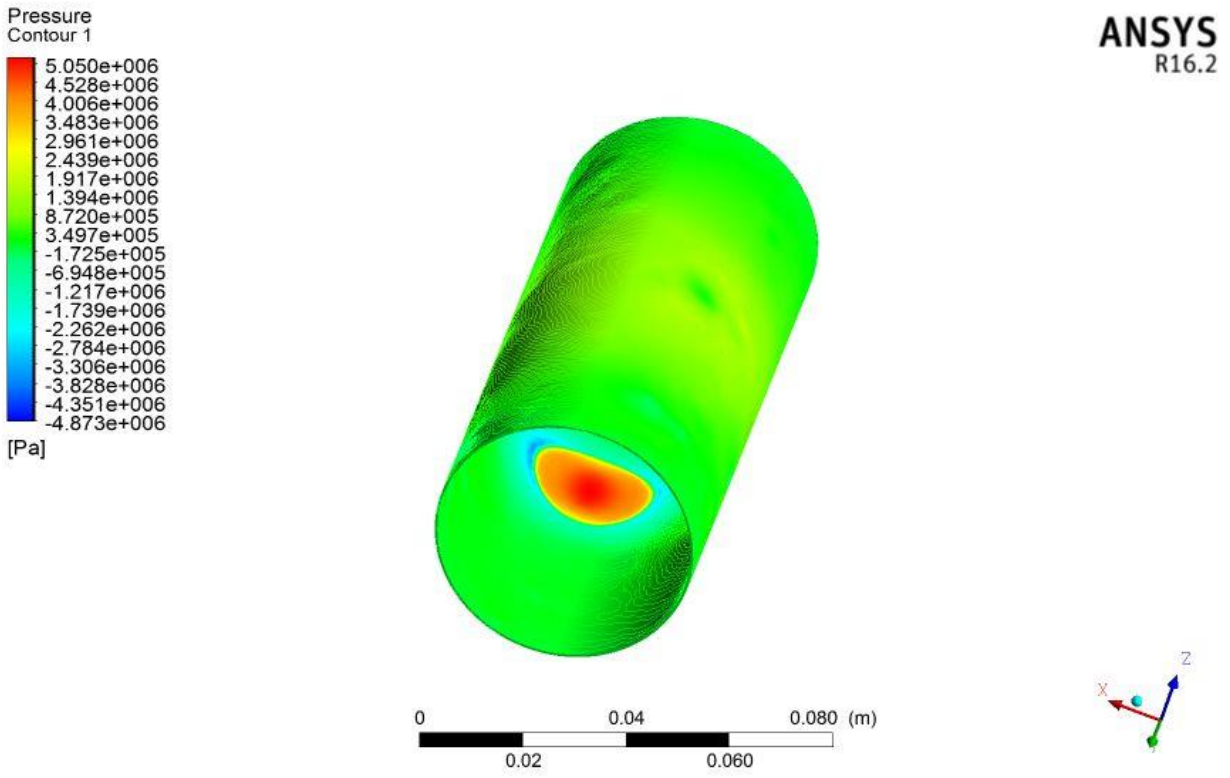

Fig. 18 Pressure contour on Journal surface with $Al_2O_3 - SAE$ 30 nanolubricant with volume fraction 0.01

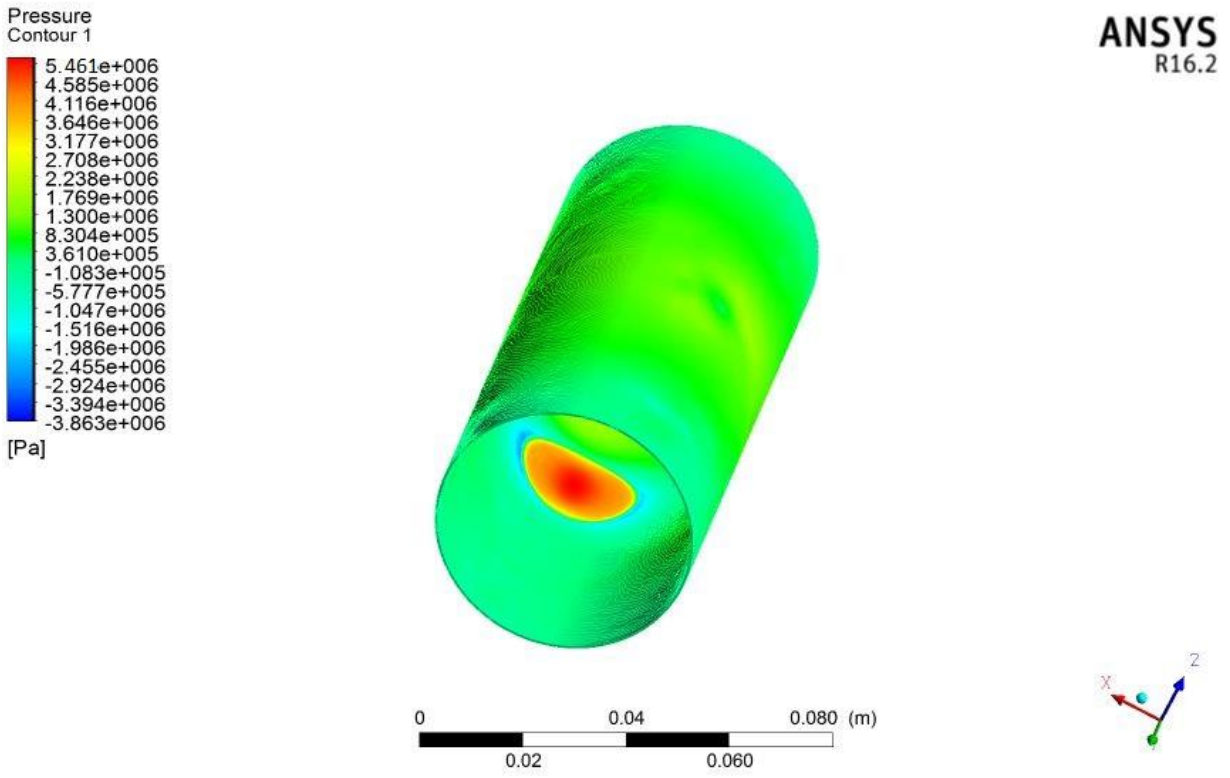

Fig. 19 Pressure contour on Journal surface with $Al_2O_3 - SAE\ 30$ nanolubricant with volume fraction 0.04

Chapter-5

Conclusion and future scope

5.1 Conclusion

Performance Analysis of Long Hydrodynamic Journal Bearing with Nano Lubricant has been carried out by developing a code in MATLAB and by using ANSYS CFD Fluid Flow(Fluent) technique for performing the pressure distribution and load carrying capacity analysis. The effects of variable density and variable specific heat on maximum pressure, load bearing, in high-speed journal bearing operation are examined. After validation of developed approach various parametric studies are conducted to examine the effects of $Al_2O_3 - SAE\ 30$ nanolubricant on the performance of long hydrodynamic journal bearing. The main contributions of present work are summarized as follows

- Journal Bearing with nanoparticle added lubricant enhances the pressure and load carrying capacity when compared with lubricant and it has optimum pressure profile with respect to $SAE\ 30$ lubricant.
- With increase in volume fraction of nanoparticle in the lubricating oil pressure carrying capacity of the hydrodynamic journal bearing increases.
- The analysis also reveals there is a decrease in friction force for lubricating oil of journal bearings using Nano lubricants, as compared to plain lubricating oil.

5.2 Future scope

In present study, performance characteristic of Long Hydrodynamic Journal Bearing are calculated using mathematical simulation and CFD simulation, however experiment based model may also be used for predicting the performance characteristic of the hydrodynamic journal bearing.

Although in present study the performance analysis of long journal bearing is carried out by assuming effect of pressure and temperature on viscosity of the lubricant are neglected and there is perfect adhesion between the lubricant and the bearing surfaces, however in practical scenario when the temperature rises, the viscosity of the lubricant decreases and affects the load capacity

of the bearing. Therefore, this analysis is useful to predict the bearing performance parameters in the actual working conditions, it may help to improve the bearing life.

References

[1] *Girard, L. Dominique (1852).* Hydraulique appliquée. Nouveau système de locomotion sur les chemins de fer (Applied hydraulics. New locomotion system for railways)

[2] Lin, J-R., R-F. Lu, and T-B. Chang. "Derivation of dynamic couple-stress Reynold's equation of sliding-squeezing surfaces and numerical solution of plane inclined slider bearings." Tribology International 36.9 (2003): 679-685.

[3] Hili, Molka Attia, et al. "Hydrodynamic and elastohydrodynamic studies of a cylindrical journal bearing." Journal of Hydrodynamics, Ser. B 22.2 (2010): 155-163.

[4] Raghavendra, N., M. C. Math, and Pramod R. Sharma. "Finite Element Method Analysis of Hydrodynamic Journal Bearing." European Journal of Advances in Engineering and Technology 2.2 (2015): 92-101.

[5] Liu, Junyan, et al. "Study on lubricating characteristic and tool wear with water vapor as coolant and lubricant in green cutting." Wear 262.3 (2007): 442-452.

[6] *Don M. Pirro; Martin Webster; Ekkehard Daschner (2016*). Lubrication Fundamentals (Third Edition, Revised and Expanded ed.). *CRC Press.* ISBN 978-1-4987-5290-9.

[7] Tiwari, Priyanka, and Veerendra Kumar. "Analysis of Hydrodynamic Journal Bearing Using CFD and FSI Technique." International Journal Of Engineering Research & Technology (IJERT) ISSN (2014): 2278-0181.

[8] Ponticel, Patrick. "SAE codifies new oil viscosity grade (SAE 16)." (2014).

[9] Singh, Kamaldeep, Sumeet Sharma, and D. Gangacharyulu. "Experimental study of thermophysical properties of Al2O3/water nanofluid." Int. J. Res. Mech. Eng. Technol. 3.2 (2013): 229-233.

[10] Choi, S.,"Enhancing thermal conductivity of fluids with nanoparticles",Development and applications of non-newtonian flows,edited by Siginer and H.P. Wang,Newyork:ASME,Vol. 12,1995,pp. 99-105.

[11] Binu, K. G., et al. "Formulation and Viscosity Analysis of TiO 2 Nanoparticle Dispersions in Engine Oil." American Journal of Materials Science 5.3C (2015): 198-202.

[12] Prabhakaran Nair, K., Mohammed Shabbir Ahmed, and Saed Thamer Al-qahtani. "Static and dynamic analysis of hydrodynamic journal bearing operating under nano lubricants." International Journal of Nanoparticles 2.1-6 (2009): 251-262.

[13] Xie, Hongmei, et al. "Lubrication performance of MoS 2 and SiO 2 nanoparticles as lubricant additives in magnesium alloy-steel contacts." Tribology International 93 (2016): 63-70.

[14] Lee, Seung Won, et al. "Investigation of viscosity and thermal conductivity of SiC nanofluids for heat transfer applications." International Journal of Heat and Mass Transfer 54.1 (2011): 433-438.

[15] Pisal, Ajinkya S., and D. Chavan. "Experimental investigation of tribological properties of engine oil with CuO nanoparticles." Int. J. Theor. Appl. Res. Mech. Eng 3 (2014): 34-38.

[16] Wu, Y. Y., W. C. Tsui, and T. C. Liu. "Experimental analysis of tribological properties of lubricating oils with nanoparticle additives." Wear 262.7 (2007): 819-825.

[17] Binu, K. G., et al. "A variable viscosity approach for the evaluation of load carrying capacity of oil lubricated journal bearing with TiO2 nanoparticles as lubricant additives." Procedia Materials Science 6 (2014): 1051-1067.

[18] Babu, Kalakada Sreedhar, K. Prabhakaran Nair, and P. K. Rajendrakumar. "Computational analysis of journal bearing operating under lubricant containing Al 2 O 3 and ZnO nanoparticles." International Journal of Engineering, Science and Technology 6.1 (2014): 34-42.

[19] Baskar, S., and G. Sriram. "Tribological Behavior of Journal Bearing Material under Different Lubricants." Tribology in Industry 36.2 (2014).

[20] Yathish, K., et al. "Study of TiO2 Nanoparticles as Lubricant Additive in Two-Axial Groove Journal Bearing." International Journal of Mechanical, Aerospace, Industrial and Mechatronics Engineering 8.11 (2014): 1723-1729.

[21] Shenoy, B. S., et al. "Effect of nanoparticles additives on the performance of an externally adjustable fluid film bearing." Tribology International 45.1 (2012): 38-42..

[22] Nehme, Gabi N. "The effect of FeF 3/TiF 3 catalysts on the thermal and tribological performance of plain oil ZDDP under extreme pressure loading." Wear 278 (2012): 9-17.

[23] Sahu, Mukesh, Ashish Kumar Giri, and Ashish Das. "Thermohydrodynamic analysis of a journal bearing using CFD as a tool." Int. J. Sci. Res. Publ 2.9 (2012): 1-7.

[24] J. S. Rao. "Rotor Dynamics 3rd Edison." New age international limited ISBN:81-224-0977-6.

[25] Shahmohammadi, P., and H. Beiki. "A numerical investigation of γ-Al2O3-water nanofluids heat transfer and pressure drop in a shell and tube heat exchanger." Transport phenomena in Nano and Micro scales 4.1 (2016): 29-35.

[26] Dhande, D. Y., and D. W. Pande. "Multiphase flow analysis of hydrodynamic journal bearing using CFD coupled Fluid Structure Interaction considering cavitation." Journal of King Saud University-Engineering Sciences (2016).

[27] Mane, Ravindra M., and Sandeep Soni. "Analysis of hydrodynamic plain journal bearing." Excerpt from the Proceedings of the 2013 COMSOL Conference in Bangalore. 2013.

[28] Evans,U. F.,Okare,E.O.,Edem. "Thermo-physical properties of selected oil samples as predictor of marine engines life span"e-ISSN: 2278-4861.volume 5,issue 2(Nov.-Dec. 2013),PP 01-06

[29] Chauhan, Amit, et al. "CFD based thermo-hydrodynamic analysis of circular journal bearing." International Journal Of Advanced Mechanical Engineering, ISSN (2014): 2250-3234.

[30] Gertzos, K. P., P. G. Nikolakopoulos, and C. A. Papadopoulos. "CFD analysis of journal bearing hydrodynamic lubrication by Bingham lubricant." Tribology International 41.12 (2008): 1190-1204.

[31] Santhanakrishnan, R., and V. Shanmugam. "Preparation and property analysis of nano-lubricant for vapour compression refrigeration system."

[32] Kedzierski, Mark A. "Viscosity and density of aluminum oxide nanolubricant." international journal of refrigeration 36.4 (2013): 1333-1340.

Appendix-A

Matlab code for pressure variation in with bearing angle in long hydrodynamic journal bearing

```
clc;
clear all;
W= 314.16;r=0.025;e=0.0006;c=2.305*10^(-3);
mu=0.0056;mu1=0.00574;mu2=0.006201;
% W is speed in rad/sec, r=journal radius in meter,e= eccentricity in meter
% mu is viscosity of lubricant SAE 30
% mu1 is the viscosity of aluminium oxide SAE 30 nanolubricant corresponding
to 0.01 volume fraction
% mu2 is the viscosity of aluminium oxide SAE 30 nanolubricant corresponding
to 0.04 volume fraction
n=e/c;
% n is eccentricity ratio
th=(0:20:180)*pi/180;
% this attitude angle
k=(6*(mu)*((r)^2)*W)/(c)^2;
y=(k*n.*(2+(n.*cos(th))).*sin(th))./((2+(n).^2).*(1+n.*cos(th)).^2);
y1=y*10^(-3);
% y1 is pressure carrying capacity of bearing in KPa corresponding to SAE 30
LUBRICANT
k1=(6*(mu1)*((r)^2)*W)/(c)^2;
y2=(k1*n.*(2+(n.*cos(th))).*sin(th))./((2+(n).^2).*(1+n.*cos(th)).^2);
y3=y2*10^(-3);
% y3 is pressure carrying capacity of bearing in KPa corresponding to
Aluminiumoxide SAE 30 NANOLUBRICANT of 0.01 volume fraction
k2=(6*(mu2)*((r)^2)*W)/(c)^2;
y4=(k2*n.*(2+(n.*cos(th))).*sin(th))./((2+(n).^2).*(1+n.*cos(th)).^2);
y5=y4*10^(-3);
% y5 is pressure carrying capacity of bearing in KPa corresponding to
Aluminiumoxide SAE 30 NANOLUBRICANT of 0.04 volume fraction
hold on;
plot(th*180/pi,y1)
plot(th*180/pi,y3,'r')
plot(th*180/pi,y5,'g')
```

Appendix-B

Matlab code for load variation in with journal speed in long hydrodynamic journal bearing

```
clc;
clear all;
L=0.125;r=0.025;
% L is length of bearing in meter
% r is radius of journal in meter
D=2*r;
% D id diameter of journal in meter
N=0:100:5000;
% N is spped of journal in r. p. m.
e=0.0006;c=2.305*(10)^(-3);mu=0.0056;mu1=0.00574;mu2=0.006201;
% e is eccentricity in meter,c is radial clearance in meter
% mu is viscosity of lubricant SAE 30
%mu1 is the viscosity of aluminium oxide SAE 30 nanolubricant corresponding
to 0.01 volume fraction
%mu2 is the viscosity of aluminium oxide SAE 30 nanolubricant corresponding
to 0.04 volume fraction
n=e/c;
% n is eccentricity ratio
z=n/((2+(n)^2)*sqrt(1-n^2));
x=((r/c)^2)*z;
y=12*pi*L*mu*(pi*D*N)./60*x;
%y is load carryin capacity corresopnding to mu viscosity  in Newton
plot(N,y);
y1=12*pi*L*mu1*(pi*D*N)./60*x;
%y1 is load carryin capacity corresopnding to mu1 viscosity in Newton
hold on;
plot(N,y1,'r');
y2=12*pi*L*mu2*(pi*D*N)./60*x;
%y2 is load carryin capacity corresopnding to mu2 viscosity in Newton
hold on;
plot(N,y2,'g')
```

Appendix-C

Report generated by ANSYS R 16.2 workbench CFD Fluid flow(Fluent)

Project

First Saved	Monday, June 19, 2017
Last Saved	Monday, June 19, 2017
Product Version	16.2 Release
Save Project Before Solution	No
Save Project After Solution	No

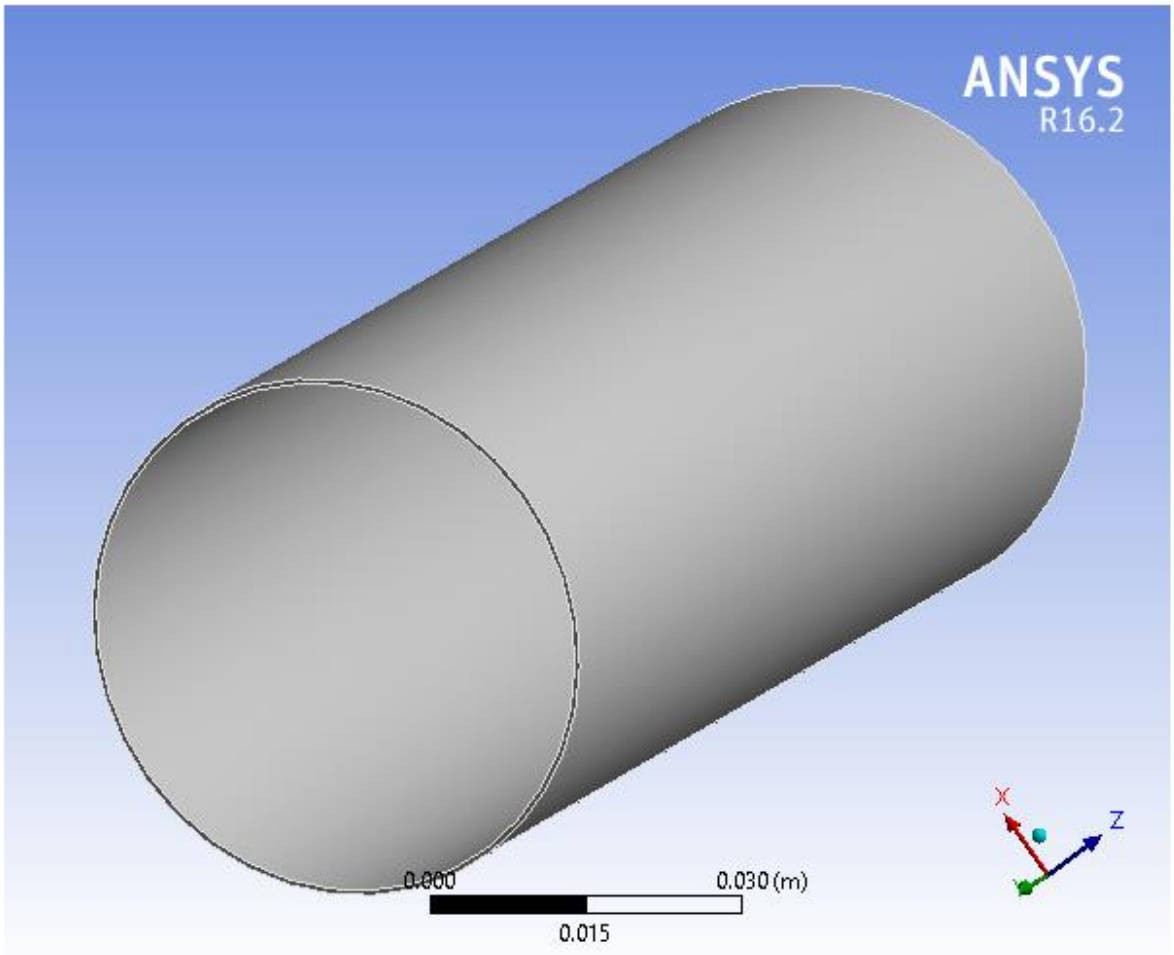
ANSYS
R16.2
0.000
0.030 (m)
0.015
X
Z

Contents

Units

TABLE 1

Unit System	Metric (m, kg, N, s, V, A) Degrees rad/s Celsius
Angle	Degrees
Rotational Velocity	rad/s
Temperature	Celsius

Model (A3, B3, C3)

Geometry

TABLE 2
Model (A3, B3, C3) > Geometry

Object Name	*Geometry*
State	Fully Defined
Definition	
Source	C:\Users\nishant srivastava\Desktop\NISHANT NEW BEARING\Final Journal Bearing\journal bearing_files\dp0\FFF\DM\FFF.agdb
Type	DesignModeler
Length Unit	Meters
Bounding Box	
Length X	5.1e-002 m
Length Y	0.125 m
Length Z	5.15e-002 m

Properties	
Volume	1.0551e-005 m³
Scale Factor Value	1.
Statistics	
Bodies	1
Active Bodies	1
Nodes	127243
Elements	480914
Mesh Metric	None
Basic Geometry Options	
Parameters	Yes
Parameter Key	DS
Attributes	No
Named Selections	No
Material Properties	No
Advanced Geometry Options	
Use Associativity	Yes
Coordinate Systems	No
Reader Mode Saves Updated File	No
Use Instances	Yes
Smart CAD Update	No
Compare Parts On Update	No
Attach File Via Temp File	Yes
Temporary Directory	C:\Users\nishant srivastava\AppData\Roaming\Ansys\v162

Analysis Type	3-D
Decompose Disjoint Geometry	Yes
Enclosure and Symmetry Processing	No

TABLE 3
Model (A3, B3, C3) > Geometry > Parts

Object Name	*PRT0004*
State	Meshed
Graphics Properties	
Visible	Yes
Transparency	1
Definition	
Suppressed	No
Coordinate System	Default Coordinate System
Reference Frame	Lagrangian
Material	
Fluid/Solid	Defined By Geometry (Solid)
Bounding Box	
Length X	5.1e-002 m
Length Y	0.125 m
Length Z	5.15e-002 m
Properties	
Volume	1.0551e-005 m^3
Centroid X	-2.3541e-018 m
Centroid Y	-4.2567e-018 m
Centroid Z	-1.7316e-003 m

Statistics	
Nodes	127243
Elements	480914
Mesh Metric	None

Coordinate Systems

TABLE 4
Model (A3, B3, C3) > Coordinate Systems > Coordinate System

Object Name	*Global Coordinate System*
State	Fully Defined
Definition	
Type	Cartesian
Coordinate System ID	0.
Origin	
Origin X	0. m
Origin Y	0. m
Origin Z	0. m
Directional Vectors	
X Axis Data	[1. 0. 0.]
Y Axis Data	[0. 1. 0.]
Z Axis Data	[0. 0. 1.]

Mesh

TABLE 5
Model (A3, B3, C3) > Mesh

Object Name	*Mesh*
State	Solved
Display	
Display Style	Body Color

Defaults	
Physics Preference	CFD
Solver Preference	Fluent
Relevance	100
Sizing	
Use Advanced Size Function	On: Curvature
Relevance Center	Fine
Initial Size Seed	Active Assembly
Smoothing	Medium
Transition	Slow
Span Angle Center	Fine
Curvature Normal Angle	Default (12.0 °)
Min Size	Default (1.4449e-005 m)
Max Face Size	7.5e-004 m
Max Size	7.5e-004 m
Growth Rate	Default (1.10)
Minimum Edge Length	3.7739e-003 m
Inflation	
Use Automatic Inflation	None
Inflation Option	Smooth Transition
Transition Ratio	0.272
Maximum Layers	5
Growth Rate	1.2
Inflation Algorithm	Pre
View Advanced Options	No

Assembly Meshing	
Method	None
Patch Conforming Options	
Triangle Surface Mesher	Program Controlled
Patch Independent Options	
Topology Checking	No
Advanced	
Number of CPUs for Parallel Part Meshing	Program Controlled
Shape Checking	CFD
Element Midside Nodes	Dropped
Straight Sided Elements	
Number of Retries	0
Extra Retries For Assembly	Yes
Rigid Body Behavior	Dimensionally Reduced
Mesh Morphing	Disabled
Defeaturing	
Pinch Tolerance	Default (1.3004e-005 m)
Generate Pinch on Refresh	No
Automatic Mesh Based Defeaturing	On
Defeaturing Tolerance	Default (7.2247e-006 m)
Statistics	
Nodes	127243
Elements	480914
Mesh Metric	None

TABLE 6
Model (A3, B3, C3) > Mesh > Mesh Controls

Object Name	*Refinement*
State	Fully Defined
Scope	
Scoping Method	Geometry Selection
Geometry	1 Face
Definition	
Suppressed	No
Refinement	2

Named Selections

TABLE 7
Model (A3, B3, C3) > Named Selections > Named Selections

Object Name	*outlet1*	*outlet2*	*inlet*
State	Fully Defined		
Scope			
Scoping Method	Geometry Selection		
Geometry	1 Face		
Definition			
Send to Solver	Yes		
Visible	Yes		
Program Controlled Inflation	Exclude		
Statistics			
Type	Manual		
Total Selection	1 Face		
Suppressed	0		
Used by Mesh Worksheet	No		